Surface temperature uniformity for single-phase developing laminar flow through horizontal tubes submerged in boiling water

Student: **Rudaviro G. Munzara**
Student No: **u20605283**
Supervisor: **Dr. Marilize Everts**

Submitted in partial fulfilment of the requirements for the degree:
Master of Science (MSc.) Applied Science Mechanics

Department of Mechanical and Aeronautical Engineering,
Faculty of Engineering, Built Environment and Information Technology
University of Pretoria,
Pretoria, 0002
South Africa

November 2022

ABSTRACT

An experimental study was done to investigate the heat transfer characteristics of simultaneously hydrodynamically and thermally developing laminar flow of water through a horizontal tube, which was submerged in boiling water to keep its surface temperature uniform. A water bath with two compartments was used to house the water at saturation whose boiling was brought about by heater elements that covered the base area of the water bath. The inside and outside diameters of the test section were 11.2 mm and 12.5 mm, respectively, and the heated length was 1 m. Experiments were conducted between Reynolds numbers of 500 and 3 000 considering different heat input levels and inlet temperatures that varied between 20 °C and 80 °C. Although nucleate pool boiling was expected to provide a uniform surface temperature, thermocouple measurements on the test section showed that the wetted surface temperatures on the inside of the test section were not uniform when the flow was still thermally developing. The surface temperatures increased and approached a constant along the length of the test section. The effects of varying the Reynolds number, the tube inlet temperatures and the heat input into the system on the surface temperatures' uniformity were investigated. In none of the tests taken were the surface temperatures sufficiently uniform although the degrees of surface temperature uniformity changed with the variation of these factors. For the first time, it has been established that the assumption of a uniform surface temperature during phase-change conditions is not valid for developing flow. From the several analyses done, it was concluded that the high heat transfer coefficients associated with developing flow significantly affected the surface temperatures' uniformity as these were found to be dominant in the entrance region. Therefore, the general assumption of a uniform surface temperature boundary condition during phase-change conditions would only be valid for fully developed flow.

PUBLICATIONS

The following article was submitted for publication in the preparation and completion of this dissertation:

R. G. Munzara, M. Everts, *Surface temperature uniformity for single-phase developing laminar flow through horizontal tubes submerged in boiling water,* International Journal of Thermal Sciences, (2022), Manuscript nr: THESCI-D-22-02639, submitted on 01/12/2022.

ACKNOWLEDGEMENTS

TABLE OF CONTENTS

LIST OF FIGURES

LIST OF TABLES

NOMENCLATURE

Symbols

A	Area	[m²]
c_p	Constant pressure specific heat	[J/kgK]
D	Diameter	[m]
g	Gravitational acceleration	[m/s²]
h	Convection heat transfer coefficient	[W/m²K]
I	Current	[A]
k	Thermal conductivity	[W/m.K]
L	Length	[m]
L_h	Hydrodynamic entrance length	[m]
L_t	Thermal entrance length	[m]
$\dot{m}$	Mass flow rate	[kg/s]
P	Pressure	[Pa]
$\dot{Q}$	Heat input	[W]
$\dot{Q}_e$	Electrical power input	[W]
$\dot{q}$	Heat flux	[W/m²]
R	Thermal resistance	[°C/W]
r	Radial distance	[m]
T	Temperature	[°C or K]
v	Velocity	[m/s]
V	Voltage	[V]
x	Local value/ Distance between two points	[m]

Dimensionless parameters

a,b,c	Constants used in correlations
Gr	Grashof number
Gz	Graetz number
Nu	Nusselt number
Pr	Prandtl number
Re	Reynolds number

Greek letters

μ	Dynamic Viscosity	[kg/m.s]
ρ	Density	[kg/m³]
v	Kinematic Viscosity	[m²/s]

Superscripts

$^{-}$	Average
m, n, p	Exponents used in correlations

Subscripts

ave	Average
b	Bulk
conv	Convection
cond	Conduction
e	Electrical
excess	Temperature difference between heater element and boiling water.
exp	Experimental
f	Film
fg	Change of state liquid to gas
FC	Forced convection
heater	Heater elements
hx	Heat transfer length
i	Inner
in	Inlet
l	Liquid
laminar	Laminar flow regime
lm	Logarithmic mean value
loss	Loss
m	Mean
MC	Mixed convection
max	Maximum
min	Minimum
n	Experimental constant
nucleate	Nucleate boiling
o	Outer
out	Outlet
s	Surface
sf	Surface-fluid property
sat	Saturation
surface	Property of a surface
x	Local value or Distance between two points
v	Vapour

1. INTRODUCTION

1.1.   Background

In designing heat exchangers, thermal engineers rely on research into the fundamentals of heat exchange and the correlations that are developed from experimentation and analysis. Heat exchangers are widely used in thermal power generation facilities, integrated heating and cooling systems, and process plants. Heat exchangers in which phase-change (boiling and condensation) occurs are critical components of the thermodynamic cycles of many clean energy facilities such as concentrated solar thermal power plants, where steam is used to drive turbines during electrical power generation [1]. However, it has been highlighted by industry experts that empirical work on heat supply by large scale solar systems is still scarce [2]. Developments in the automotive industry also require improved cooling systems and increased radiator efficiencies for continued improvement in vehicle performance [3]. Cool air ventilation in deep shaft mining, where rock temperatures can reach up to 90 °C, is made possible using sophisticated phase-change heat exchanger technology, which also requires further improvement for efficiency through scientific research [4]. A thorough understanding of the heat transfer fundamentals associated with these components is thus necessary for further development and implementation.

Depending on the application, heat exchangers can be designed to operate with fluids in different flow regimes that are either laminar, transitional or turbulent. The laminar flow regime is generally associated with lower heat transfer rates and lower pressure drops. The difference between the laminar and turbulent fluid flow regimes is determined by the ratio of the inertial to the viscous forces that are dominant in the flow [5]. The convection characteristics of laminar flow are very sensitive to the temperature distribution of the wetted surfaces in the direction of flow. Internal convection heat transfer is thus analysed by first determining if there is either a uniform surface temperature or a uniform heat flux boundary condition [5]. For accurate analysis, it has been accepted that the wetted surface temperatures on the inside of the test section are to be used in the data reduction and analysis of internal flow through heat exchangers [5-8].

Several experimental studies have been done on the uniform surface temperature boundary condition using a variety of experimental setups [9-15]. This boundary condition is generally believed and assumed to occur when there is saturation or phase-change on the outer surface of a test section, or when using a tube-in-tube heat exchanger with high annular flow rates. The effects of free convection are also critical in internal flow as these can increase the heat transfer in laminar flow by a factor up to four. Thus, a thorough understanding of the experimental set-up employed, the test fluid used and the respective assumptions made in analysis is needed in order to draw useful conclusions from any experimentation with laminar flow. The literature explored mostly covered the uniform surface temperature thermal boundary condition for fully developed laminar flow and very few cover the developing flow.

1.2.   Problem statement

Although a uniform surface temperature has been generally assumed in previous studies for laminar flow through horizontal tubes, no information was found on the degree of uniformity of the surface temperatures when flow was hydrodynamically and thermally developing. No detailed experimental study nor analyses has been done on how the wetted surface temperatures on the inside of the test section develop along the tube length and the factors that affect them. However, although it was not the focus of their studies, some researchers did recommend deeper research into this phenomenon [16-18].

1.3.   Aim

The purpose of the study was thus to investigate the inner surface temperature uniformity for internal single-phase developing laminar flow through a horizontal tube exposed to nucleate pool boiling on the outer surface.

1.4.   Objectives

The main objectives of the study were:

i.   to establish the tube's wetted surface temperature development and uniformity for simultaneously thermally and hydrodynamically developing laminar flow through a tube submerged in boiling water;

ii.   to study the effects of Reynolds number on surface temperature uniformity in developing laminar flow;

iii.   to establish the effects of tube inlet temperatures on the surface temperature uniformity in developing laminar flow;

iv.   to determine the effect of heat input into system on the surface temperature uniformity in developing laminar flow and the whole thermal system;

v.   to determine the heat input conditions required to sustain a uniform surface temperature thermal boundary condition.

1.5.   Overview of dissertation

In Chapter 2 a literature review is given on the state of the art of experimental studies using a uniform surface temperature boundary condition. Relevant thermal principles and parameters of importance are also discussed in this section. Chapter 3 gives details of the experimental setup employed, the experimental matrix, the data reduction methodology and the uncertainty analysis done. The validation of the experimental setup and data reduction method was detailed in Chapter 4. The results and thermal analysis are discussed in Chapter 5 as per the stated objectives. Chapter 7 details the conclusions and recommendations for further works. Appendix A provides details on the calibration methodologies employed, while Appendix B describes the uncertainty analysis of the instrumentation used and the various correlations employed in data reduction.

2. LITERATURE REVIEW

2.1. Introduction

This chapter provides a framework of fluid flow and relevant heat transfer fundamentals. The non-dimensional parameters which are calculated in analysis are discussed as well as the importance of thermal boundary conditions in internal laminar flow. Experimental studies and heat transfer correlations developed in past studies are also critically analysed, with careful considerations made for the differences in conditions during the respective experiments. Gaps of information in available literature are cited throughout this chapter, building up to the aim and objectives of the study.

2.2. Non-dimensional parameters

2.2.1. Reynolds number

After conducting experiments using dye in flow through glass tubes in the 1980s, Osborn Reynolds concluded that a flow regime is dependant mainly on the ratio of a fluid flow's inertial forces to its viscous forces [19]. This ratio became known as the Reynolds number.

$$Re = \frac{\rho v D}{\mu} \tag{2.1}$$

Conventionally it is accepted that, if

- Re < 2 300, the flow will be laminar with the viscous forces (friction) more dominant that the random inertial forces.
- Re > 10 000, the fluid assumes fully turbulent flow where the convection (or inertial) forces are dominant causing fluctuations in the fluid.
- 2 300 < Re < 10 000, the fluid flow will be transitioning from laminar to a fully turbulent flow. This usually cited range, however, applies strictly to a very steady and uniform entry flow with a rounded entrance [5].

2.2.2. Prandtl number

For laminar flow in a tube, the Prandtl number is a measure of the growth of the velocity boundary layer relative to the thermal boundary layer [5]. It can also be defined as the ratio of viscous diffusion over thermal (heat) diffusion, a value that depends on temperature [19].

$$Pr = \frac{\mu c_p}{k} \tag{2.2}$$

It should be noted that if,

- $Pr \approx 1$, the velocity and thermal boundary layers essentially coincide with each other, as with flow in gases.
- $Pr >> 1$, the velocity boundary layer outgrows the thermal boundary layer as the rate of change of momentum is faster than that of heat, typical of oils.
- $Pr << 1$, the thermal boundary layer outgrows the velocity boundary layer, as with liquid metals, implying that the hydrodynamic entry length will be longer than thermal entry length.

3

2.2.3. Nusselt number

The Nusselt Number represents how heat transfer through a fluid layer is enhanced due to convection relative to conduction across the same flow [5].

$$Nu = \frac{hD}{k} \qquad (2.3)$$

Cengel and Ghajar [5] noted that there is a limited number of empirical correlations available for the Nusselt number for laminar flow under uniform surface temperature boundary conditions.

2.2.4. Grashof and Rayleigh numbers

The Grashof number, *Gr*, expresses the significance of the buoyancy forces due to the thermal gradients compared to the opposing viscous forces. Furthermore, the Rayleigh number, *Ra*, is the product of the Grashof number and Prandtl number for the different fluids [19]. Their magnitudes give indications of whether flow is dominated by mixed or forced convection which is critical in determining secondary flow effects. They are respectively given as:

$$Gr = \frac{\rho^2 \beta (T_s - T_m) D^3}{\mu^2} \qquad (2.4)$$

$$Ra = \frac{\rho \beta (T_s - T_m) L^3}{\mu \alpha} = GrPr \qquad (2.5)$$

where β is the expansion coefficient.

2.2.5. Graetz number

This parameter is used to determine whether the flow is fully developed or not. It is asserted that for values greater than $1/Gz \approx 0.05$, for flow under either uniform heat flux or uniform surface temperature boundary conditions, the flow is fully developed [5].

$$Gz = \left(\frac{D}{x}\right) RePr \qquad (2.6)$$

The local values of Nusselt number are sometimes presented either graphically and/or in tabular form in terms of the inverse of the Graetz number.

2.3. The Basics of laminar flow

Laminar flow is when fluid particles flow in parallel layers without lateral mixing. There are no crosscurrents perpendicular to the direction of flow as the adjacent layers slide between one another (no swirls). Cengel and Ghajar [5] describe it as flow with smooth streamlines and highly ordered motion. Newtonian fluids obey Newton's Law of viscosity which states that shear stress is directly proportional to rate of shear strain. It thus follows that laminar flow occurs when viscous forces (dependant on velocity gradient and viscosity) are stronger than the inertial forces (dependant on the density and velocity of flow) [5]. It is generally accepted that internal flow is laminar when the Reynolds number is less than 2 300.

2.4. Forced and mixed convective flow

Forced Convection occurs when the fluid motion through a hot or cold tube is caused by a pump (or fan for gases). It can also be termed imposed flow. For this type of flow, the velocity of the fluid is high enough to suppress secondary flow and natural convection is negligible. One of the traits of forced convection is that heat transfer is enhanced by the fluid velocity [18, 19].

4

Mixed convection is when the fluid motion is due to both applied pressure forces and buoyant forces. It can also be termed as combined natural and forced convection. Typical of natural convection, the free convection effects due to temperature and buoyancy differences remain significant, which leads to secondary flow. Whenever heat is transferred into a fluid, the local temperature will change resulting in a change in density (in relation to the surrounding fluid).

(a) (b)
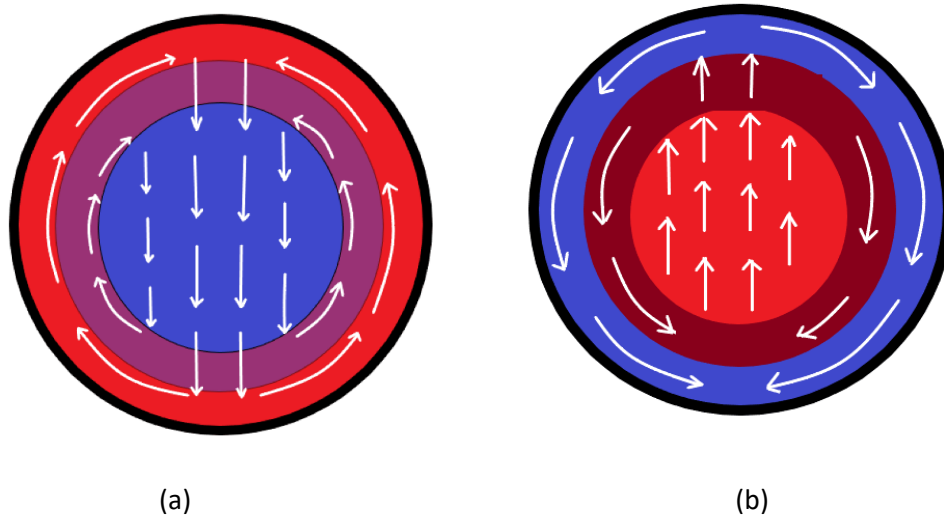
Fig. 2.1: Schematic representation of counter-rotating vortices as a result of free convection during (a) heating and (b) cooling respectively.

As schematically indicated in Fig 2.1 it has been established that when a fluid flows at relatively low flow rates through a heated tube, the fluid near the wetted surface circulates upwards (opposite direction to gravity), as it will be at a higher temperature and lower density [20]. The fluid near the centre of the test section flows downwards as it will be at a lower temperature and higher density, according to the principles of continuity. This leads to a secondary fluid motion, which is also known as free convection. The flow circulations will be in the opposite direction when the tube is being cooled. Depending on prevalent conditions during flow, these effects may not always be significant [5]. The flow regime maps of Metais and Eckert [21] developed for the uniform surface temperature boundary condition can be used to predict whether there is purely forced convection or mixed convection in laminar flow. Mixed convection is very important to consider as free convection effects can increase the heat transfer in laminar flow by a factor up to four and have notable effects on the fluid flow characteristics [12].

2.5.   Thermal boundary conditions

It is accepted in literature that the heat transfer coefficients and pressure drop characteristics for a fully developed laminar flow in a circular tube differ depending on the boundary conditions applicable. The same boundary conditions exist in practical applications of heat exchangers. The surface conditions can be approximated to be uniform surface temperature (T_s = constant) or uniform surface heat flux ($\dot{q}_s$ = constant) [5].

2.5.1.   Uniform heat flux

Realised when the tube is subjected to a uniform radiation or electric resistance, the uniform surface heat flux can be expressed as:

$$\dot{q}_s = h(T_s - T_i) = \frac{\dot{Q}}{A_s}$$

(2.7)

5

where *h* was the heat transfer coefficient, T_s the surface temperature and T_i was the mean water temperature inside the test section.
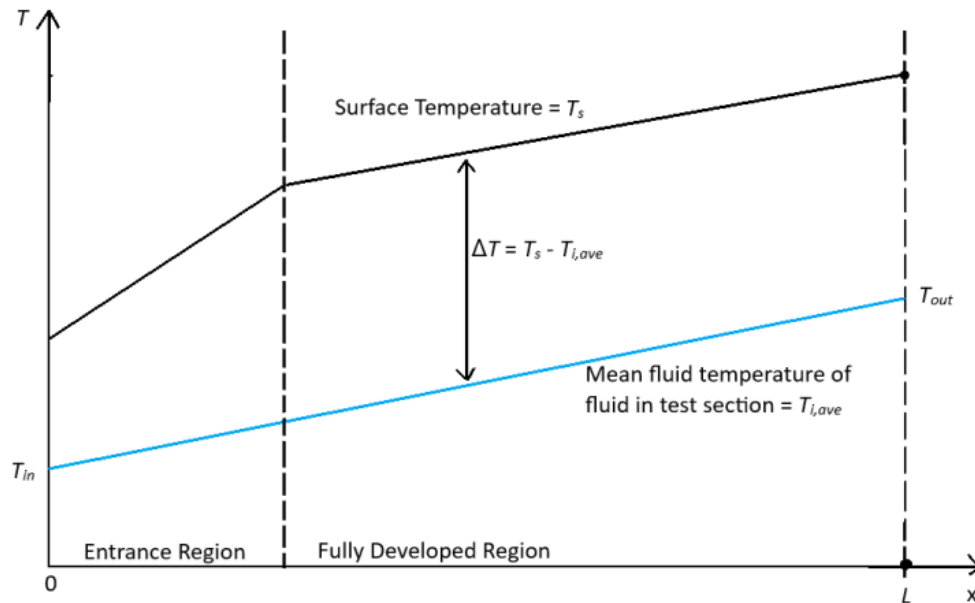
Fig. 2.2: Variation of the tube surface and the average fluid temperatures along the test section for a uniform heat flux thermal boundary condition. Figure adapted from Cengel and Ghajar [5].

As schematically indicated in Fig. 2.2, the average fluid temperature increases linearly in the direction of flow due to a linear increase of surface area across the tube length and the uniform heat input per surface area. The surface temperatures also increase along the tube length, but the surface-fluid temperature difference only becomes constant once the flow is fully developed. Therefore, it can be concluded that for fully developed flow, the temperature gradient is independent of axial position (no axial heat transfer) and effectively the temperature profile does not change along the tube [5]:

$$\frac{\partial T}{\partial x} = \frac{dT_s}{dx} = \frac{dT_m}{dx} = \frac{\dot{q}_s p}{\dot{m}c_p} = constant \tag{2.8}$$

After analysis of the above equations, it has been accepted in literature that for fully developed laminar flow in a circular tube subjected to a uniform heat flux, *Nu* = 4.36.

2.5.2. Uniform wall temperature

This boundary condition is realised when the surface temperature of a tube is maintained uniform, typical of when a phase change occurs at the outer surface of the tube [5]. Other researchers have employed test sections made up of tube in tube heat exchangers with high velocity flow in the annular passage to achieve uniform wall temperature conditions on the inner tube.
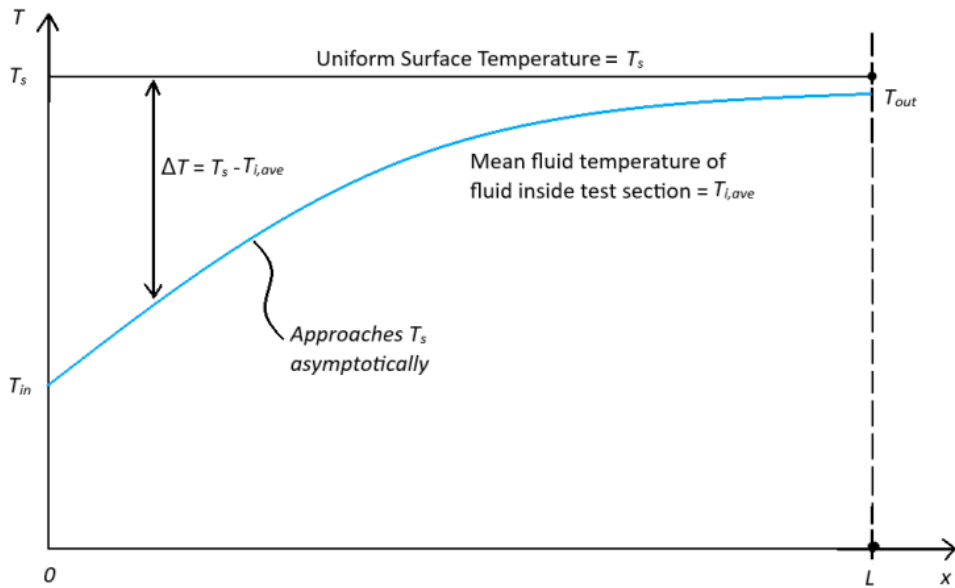
Fig. 2.3: The variation of average fluid temperature along the test section for a uniform surface temperature thermal boundary condition. Figure adapted from Cengel and Ghajar [5].

The bulk fluid temperature increases logarithmically along tube length, as indicated in Fig. 2.3 and the heat transfer rate can be expressed as:

$$\dot{Q} = hA_s\Delta T_{avg} = hA_s\Delta T_{lm} \qquad (2.9)$$

where T_{lm} is the log mean temperature difference between the surface and the fluid given by:

$$\Delta T_{lm} = \frac{T_{in} - T_{out}}{\ln\left(\frac{T_s - T_{out}}{T_s - T_{in}}\right)} \qquad (2.10)$$

It has been asserted that the log mean temperature difference is the most reliable value of the average temperature difference between the fluid and the tube surface as it can be used for both heating and cooling and is practically failsafe if T_e and T_i are used interchangeably (only the sign will change but not the magnitude) [5]. It also truly represents an exponential decay of the local temperature difference between the fluid and the surface, as indicated in Fig. 2.3. It has been established that the Nusselt number for fully developed laminar flow subjected to a uniform wall temperature boundary condition is $Nu = 3.66$, which is 16% less than that of flow under uniform heat flux.

7

2.6. Experimental studies on laminar flow with a uniform surface temperature thermal boundary condition

Several experimental studies have been done on the uniform surface temperature boundary condition using a variety of experimental setups. This thermal boundary condition is generally believed and assumed to occur when there is saturation or phase-change on the outer surface of a test section or when using a tube-in-tube heat exchanger with high annular flow rates [5, 22].

Table 2.1 details relevant experimental studies on forced and mixed convective laminar flow through horizontal test sections with a uniform surface temperature boundary condition. In their analysis of the state of the art on the science, Yousef and Tarasuk [15] give an excellent comparative account of the different Nusselt number correlations presented. The differences between the studies were largely attributed to the differences in the mentioned prevalent conditions during experimentation and data reduction.

To develop a forced convection Nusselt number correlation, Colburn [9] considered a test section configuration which involved the condensation of steam from saturated air streams in the annular passage. He asserted that during the thermal analysis, the mean film temperature, T_f, was to be employed and the properties of the test fluid were to be evaluated at the same temperature to account for viscosity of the fluid. Thus, the viscosity correction ratio μ_f / μ_b was introduced in Eq. (2.11) for the streamline region, where the bulk fluid temperature was obtained from the average of the inlet and outlet temperatures. The saturation temperature on the outside of the test section was considered as the surface temperature of the test section in the data reduction and analysis.

Sieder and Tate [10] made use of a heavily insulated concentric tube-in-tube heat exchanger. Manual effort and adjustment were performed to keep the surface temperatures of the inner tube uniform for the respective flow rates within a short period of time. They noted a lack of agreement between their heat transfer correlation and those in literature, due to differences in the magnitude of the exponents used in the Reynolds number, Prandtl number and viscosity groups. However, they provided for easier manipulation of the Colburn [9] equation by using the expression $(\mu_b/\mu_s)^{0.14}$ to account for the radial variation of fluid properties [12].

After a macroscopic analysis of their system, Jackson et al. [11] developed a Nusselt number correlation for the uniform surface temperature boundary condition, using air as the test fluid in a tube-in-tube experimental setup. They suggested the elimination of the term L/D from the free convection term. The L/D ratio had been initially introduced by Eubank and Proctor [23] in their Nusselt number derivations from experiments using heavy oils, which were characterised by a high viscous to buoyancy ratio [23]. To maintain a uniform surface temperature, Oliver [12] used a water jacket. His results showed that the effects of free convection increased along the test section's length. In their investigations on free and forced convection for laminar flow in horizontal tubes, Brown and Thomas [13] obtained experimental data that did not agree with existing correlations, which had been mainly developed using oils at the time. Therefore, they developed Eq. (2.15) which fitted their water data within ±8%.

8

Table 2.1: Data and correlations obtained from experimental studies on forced and mixed convective laminar flow through horizontal test sections with a uniform surface temperature boundary condition

Authors	Year	Correlation	Eq.	Fluid	Experimental Setup	Prandtl numbers	Reynolds numbers	Surface temperature range [°C]	Temperature Gradient [°C/m]	Total thermo-couples	L/D	Developing/ Fully developed	Convection Type	Uncer-tainty	Other Conditions
Colburn [9]	1933	$Nu\left(\frac{\mu_f}{\mu_b}\right)^{1/3} = 1.75\,Gz^{1/3}\left[1 + 0.015\,Gr_f^{1/3}\right]$	(2.11)	Air, Light oils	Condensation of steam in annuli	0.76 - 160	300 −25 000 Laminar - Turbulent	-	-	-	24 - 400	Fully developed	Forced	-	Fluid properties evaluated at film temperature
Sieder and Tate [10]	1936	$Nu = 1.86\left(\frac{RePrD_i}{L}\right)^{1/3}\left(\frac{\mu_b}{\mu_s}\right)^{0.14}$	(2.12)	Oils, Water	Tube-in-tube (annulus)	0.6 - 5	≤ 2400	-	-	5	81.58	Fully developed	Forced and mixed	-	Heating and cooling $0.0044 \le (\mu_b/\mu_s) \le 9.75$
Jackson et al. [11]	1961	$Nu = 2.67[(Gz_b)^2 + (0.0087)^2(Gr_{lm}Pr)_w^{1.5}]^{1/6}$	(2.13)	Air	Steam tank	0.71	1 300 -2 300	98	-	6	-	Developing flow	Mixed	±5%	Correlation is semi-theoretical
Oliver [12]	1962	$Nu\left(\frac{\mu_w}{\mu_b}\right)^{0.14} = 1.75\left[Gz + 5.6\times10^{-4}\left(GrPr\frac{L}{D_i}\right)^{0.7}\right]^{1/3}$	(2.14)	Water, Ethyl-alcohol, Glycerol -water	Water jacket	4.32 − 9.5, 4.8 − 7.0, 62 - 326	141 -1 580	7.0 − 39.1, 9.0 − 39.3, 9.8 − 41.2	1.09	4	72	Fully developed	Mixed	±6%	Correlation is invalid when Gz x m < π x Nu
Brown and Thomas [13]	1965	$Nu\left(\frac{\mu_w}{\mu_b}\right)^{0.14} = 1.75\left[Gz + 0.012(GzGr^{1/3})^{4/3}\right]^{1/3}$	(2.15)	Water	Water Jacket	3.5 − 7.4	235 −1 240	46.8 − 91.5	1.09, 0.72	-	36 − 110	Fully developed flow at the onset of heating.	Mixed	-	Based on arithmetic temperature difference and not LMTD
Depew and August [14]	1971	$Nu\left(\frac{\mu_w}{\mu_b}\right)^{0.14} = 1.75\left[Gz + 0.12(GzGr^{1/3}Pr^{0.36})^{0.88}\right]^{1/3}$	(2.16)	Water, Ethyl-alcohol, Glycerol -water	Vapour compression cycle	5.7 − 8.0	316 −1 810	47.6 − 49.1, 46.1 − 47.6, 48.6 − 51.1	2.94	8	0.566	Fully developed	Mixed	±2%	Based on arithmetic temperature difference and not LMTD
Yousef & Tarasuk [15]	1982	$Nu\left(\frac{\mu_w}{\mu_b}\right)^{0.14} = 1.75\left[Gz + 0.245(Gz^{1.5}Gr^{1/3})^{0.882}\right]^{1/3}$	(2.17)	Air	Electrical heating wire wrapped in spiral grooves of segments of the test section	0.5	138 −1 179	40.1 − 131.6	4.38	3 per segment	14 - 46	Thermally and hydrodynamically developing.	Forced and mixed	-1.5% and +4%	Based on LMTD method.

Depew and August [14] studied forced and mixed convective flow in relatively short horizontal tubes with *L/D* = 28.4. They introduced the Prandtl number to account for large viscosity variances in some fluids. Their equation correlated to other water data within ±40% but was said to be applicable to a variety of other fluids for different heating and cooling conditions. Using air as the test fluid, Yousef and Tarasuk [15] experimentally proved that free convection in horizontal tubes does not depend on the *L/D* ratio, a conclusion that had also been drawn by Depew and August [14] and Brown and Thomas [13] who used heavier and more viscous fluids. Yousef and Tarasuk [15] also showed that free convection is rather dependent on the Grashof and Graetz numbers and can enhance heat transfer by factors up to 2.5 compared to the forced convection predictions. However, when correlating the local Nusselt numbers, Nu_x, significant deviations were observed, and an error analysis of their experimental data gave an uncertainty of ±20%. This indicated the need for further study and research into the matter.

However, it is important to note that only two of the research studies [11, 15] presented in Table 1 have results for simultaneously thermally and hydrodynamically developing laminar flow. Meyer and Olivier's [17] measured surface temperatures in developing laminar flow under a uniform surface temperature boundary condition showed a temperature difference of 3 °C between the maximum and minimum measured wetted surface temperatures over tube lengths of 5 m. Their findings on laminar friction factors and heat transfer results were also different from the theoretically predicted values. They highlighted the need for further investigation into the surface temperature development as well as the effects of free convection in the laminar flow regime. It was interestingly noted that none of the other related studies in literature gave detail on how the surface temperatures developed with increase in heat transfer area along the respective test sections' lengths.

2.7. Analytical studies on laminar flow with a uniform surface temperature thermal boundary condition

Graetz was amongst the first researchers to mathematically analyse heating and cooling of fluid flow through a horizontal tube at constant mass rate in undistorted streamline flow [24, 25]. To characterise the velocity and thermal development of flow he suggested that the change in bulk temperature ΔT_i was a product of a series function of the dimensionless group $\left(\frac{\dot{m}c_p}{kL}\right)$ and the initial temperature difference between the fluid and the tube surface. Other numerical research studies on heat transfer in developing and fully developed laminar flow with a uniform wall temperature are available in literature [26-31]. The most recent analytical work on the Graetz problem for laminar flow in round pipes has been done by Bennet [24, 25] who proposed Nusselt number correlations with errors within -3.0% and +1.2% of theoretical isothermal pipe flow calculations. However, only correlations developed from experimental data were considered in the data reduction and analysis.

2.8. Limitations of laminar flow with a uniform wall temperature boundary condition

The following few cases are part of extensive research of work done on laminar flow with a uniform heat flux boundary condition. The works are mentioned to highlight the deficiency in typical data and information to solve the uniform wall temperature problem.

Mohammed and Salman did a study on the local and average heat transfer for developing and fully developed laminar mixed convective flow of air through a horizontal circular cylinder and concluded that the free convection effects tend to decrease the heat transfer results at low Reynolds numbers while they increase the heat transfer results for high Reynolds numbers [32]. Mohammed et al. [33] later did an experimental study on the effects of forced and free convective heat transfer for thermally developing and fully developed laminar flow of air inside a horizontal concentric annulus in the

thermal entrance length. The inner wall had a uniform heat flux boundary condition, while the outer annular wall was insulated. The investigation covered flow of $200 < Re < 1000$ and $6.2 \times 10^5 < Gr < 1.2 \times 10^7$. They found that buoyancy-driven secondary flow significantly increased the heat transfer coefficients. The heat transfer coefficients for thermally developing flow were considerably greater than the corresponding values for fully developed flow for a good part of the annulus [33]. Meyer and Everts [34] concluded that forced convection conditions seldom exists in practice and that the majority of the applications contain mixed convective flow.

Islam et al. [35] conducted numerical and experimental investigations on the steady laminar mixed convection heat transfer in the entrance region of horizontal annuli using air and water. The surfaces boundary conditions employed were that of a uniform heat flux at the inner wall and an adiabatic outer wall. The numerical study was conducted within the annular diameter range of 0.10 to 0.67 and $200 < Re < 1000$. They found out that buoyancy influenced the development of axial flow and temperature field with its effects being more pronounced at the inlet section where the flow was characterised by deceleration and acceleration of axial flow at the upper and lower parts of the annulus respectively. The same influence increased with increased Rayleigh number. However, further downstream, the interaction between axial flow and secondary flow became weaker [35].

Recently, a significant body of research has been conducted at the University of Pretoria on developing and fully developed forced and mixed convective flow through tubes heated at a uniform heat flux [17, 20, 22, 34, 36-40]. Meyer and Everts found that for simultaneously thermally and hydrodynamically flow, a longer thermal entrance length is required than when the flow is hydrodynamically fully developed [20, 34]. Furthermore, it was also found that free convection effects led to a decreased thermal entrance, but an increased hydrodynamic entrance length [20]. Apart from developing local and average Nusselt number correlations for developing and fully developed mixed convective laminar flow Meyer and Everts also developed uniform heat flux boundary condition flow regime maps for both high and low Prandtl number fluids for a wide range of tube diameters [38]. These are considered the latest and most reliable flow regime maps for the following reasons:

• They contain contour lines that show the Nusselt number enhancements due to the effects of free convection as expected.
• They were developed as a function of temperature difference (Grashof number) and heat flux (modified Grashof number).
• Four of the six flow regime maps are valid for both fully developed and developing flow.

Although it is very challenging to obtain forced convection conditions, Bashir et al. [36, 40] were able to investigate forced and mixed convective flow by making use of horizontal, inclined and vertical tubes. Among their findings were that the fully developed laminar forced convection friction factors were, as expected, equal to $64/Re$ but a revised laminar Nusselt number correlation for smooth circular tubes had to be developed. This was due to the fact that for Reynolds numbers greater than 1000, the Nusselt numbers were functions of the Reynolds number and no longer uniform at the theoretical Nusselt number of 4.36.

It should be noted, however, that the extensive research and attention that has been given to the uniform heat flux thermal boundary condition has not been on equal scale, but much more than the work done for uniform surface temperature. It is therefore clear that valuable contributions to the fundamental understanding of developing and fully developed forced and mixed convective laminar flow were made during the past decade. However, there findings were obtained when using tubes heated at a uniform heat flux and might not necessarily be transferable to tubes maintained at a

11

uniform temperature, due to significantly different temperature profiles that exist for these two boundary conditions (as illustrated in Fig. 2.2 and Fig. 2.3).

2.9.   Conclusions

This chapter gave an overview of the relevant fundamental heat exchange and internal fluid flow principles. Applicable non dimensional parameters, the basics of laminar flow and thermal boundary conditions were discussed in detail. It was established that the laminar flow is highly sensitive to the prevalent thermal boundary condition. Much attention was paid to previous experimental studies on laminar flow under the uniform surface temperature thermal boundary condition with the differences in the conditions during experimentation clearly stated in order to give a fair comparison of the studies and allow for better conclusions to be made.

Although heat exchange with a uniform surface temperature boundary condition has been studied by several researchers, none of the previous studies detailed how the wetted surfaces on the inside of the test section developed with increase in heat transfer area, especially in the developing region where high heat transfer coefficients are dominant. Valuable contributions have been made in the recent years to improve our fundamental understanding of forced and mixed convective developing and fully developed flow in the laminar flow regime. However, it was established that most of these studies were conducted using tubes heated at a uniform heat flux. Due to the significantly different temperature profiles that exist in tubes heat at a uniform heat flux and tubes maintained at a uniform temperature, it is important that similar research is also conducted for a uniform temperature boundary condition.

12

3. EXPERIMENTAL SETUP AND DATA REDUCTION

3.1. Introduction

This chapter describes the experimental set-up which was employed to conduct the needed heat transfer experiments with a horizontal test section immersed in boiling water. An overview of the components, materials and instrumentation used in experimentation is given, stating the function and importance of each. The test matrix, experimental procedure, data reduction method and uncertainty analysis are also discussed.

3.2. Experimental setup

The basic layout of the experimental setup used is shown in Fig. 3.1. A 1 000-litre storage tank was connected to a thermostat-controlled bath that ensured a constant fluid temperature at the inlet of the test section. Water was used as the test fluid and was pumped through the test section using a positive displacement pump. The test section was made of a 1 m long hard-drawn copper tube with inside and outside diameters of 11.2 mm and 12.5 mm, respectively. The mass flow rate of water through the test section was controlled by variable frequency drives connected to the pump. A 4-litre accumulator, with an air-filled rubber bladder, was used to dampen any flow fluctuations that may have been caused by the pump, ensuring a constant pressure and mass flow rate at the test section's inlet.
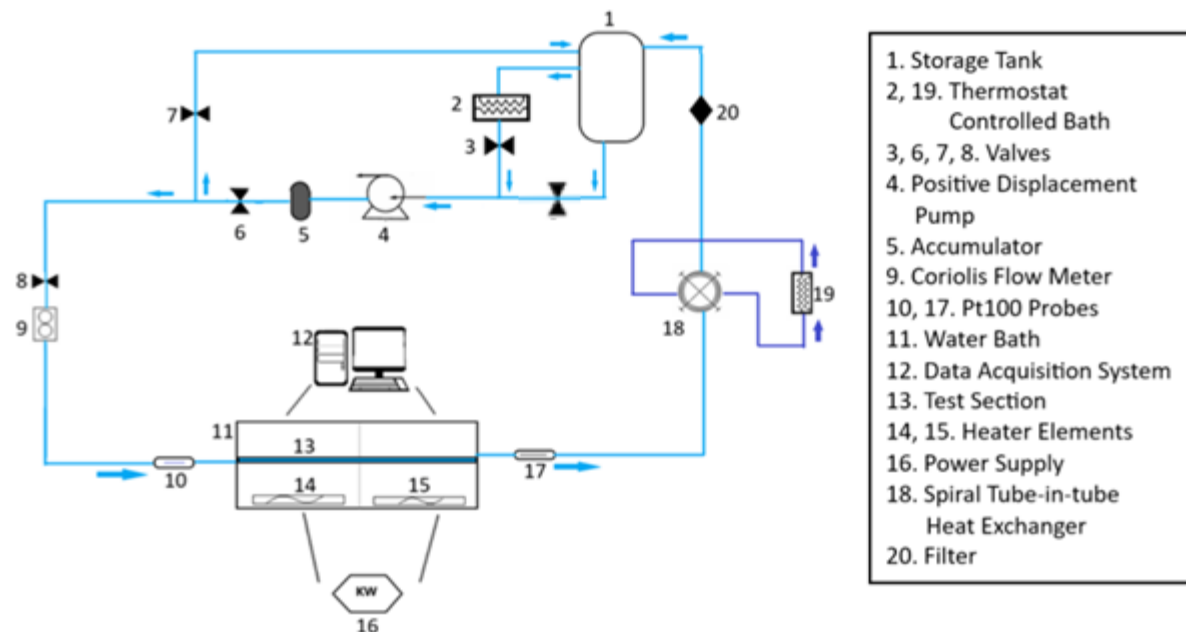
Fig. 3.1: Schematic of the experimental setup used to conduct heat transfer measurements.

In-between the accumulator and the Coriolis flow meter was a bypass valve that allowed water to flow back into the storage tank. Adjusting the bypass and supply valves allowed the backpressure on the pump to be increased while maintaining a constant flow rate to the test section. This was done to prevent increased pulsations at low pump speeds [41]. The Coriolis flow meter had a range of 0 - 0.604 kg/s and an accuracy of ±0.05%. A secondary closed loop system made up of a cooling coil and a thermostat-controlled bath was used to cool the hot water flowing from the test section before reaching the storage tank.

13

The Data Acquisition System was used to record data from the flow meters, thermocouples and Pt100 probes. It consisted of the Signal Conditioning eXtensions for Instrumentation (SCXI) hardware and a personal computer that used the National Instruments LabVIEW software to take measurements. The SCXI hardware included multiplexers, terminal blocks and analogue to digital converters. Once steady state conditions were reached, a total of 200 data points at 10 Hz were logged and then averaged to produce a single experimental measurement. The measured data were then analysed using various software that included Python, Engineering Equation Solver (EES) and Microsoft Excel.

3.3. Uniform surface temperature water bath

One of the major challenges when conducting experiments using a uniform surface temperature boundary condition, is to determine the mean fluid temperatures without obstructing the flow. The copper plate dividing the two compartments of the water bath (Fig 3.2) made it possible to conduct separate boiling experiments in either half of the test section. Tests were thus done on 0.5 m and 1 m lengths of the test section inside the water bath. When conducting experiments using the first compartment only, the second compartment was emptied, and the test section was well insulated using 120 mm thick Armaflex Class 0 insulation. The fluid temperature measured by the Pt100 probe at the outlet of the second compartment was then used as the fluid temperature at the outlet of the first compartment (because the heat losses in the second compartment were considered to be negligible). This made it possible to obtain the mean fluid temperature at x = 0.5. The dimensions of each compartment were 0.5 m x 0.25 m x 0.3 m. A copper plate lid with two 60 mm diameter vents was used to cover the water bath, control the rate of evaporation, and route the thermocouples from the test section to the Data Acquisition System. The outside of the water bath was insulated using Armaflex Class 0 insulation (thermal conductivity of 0.033 W/mK) to limit heat losses to the ambient air during testing.
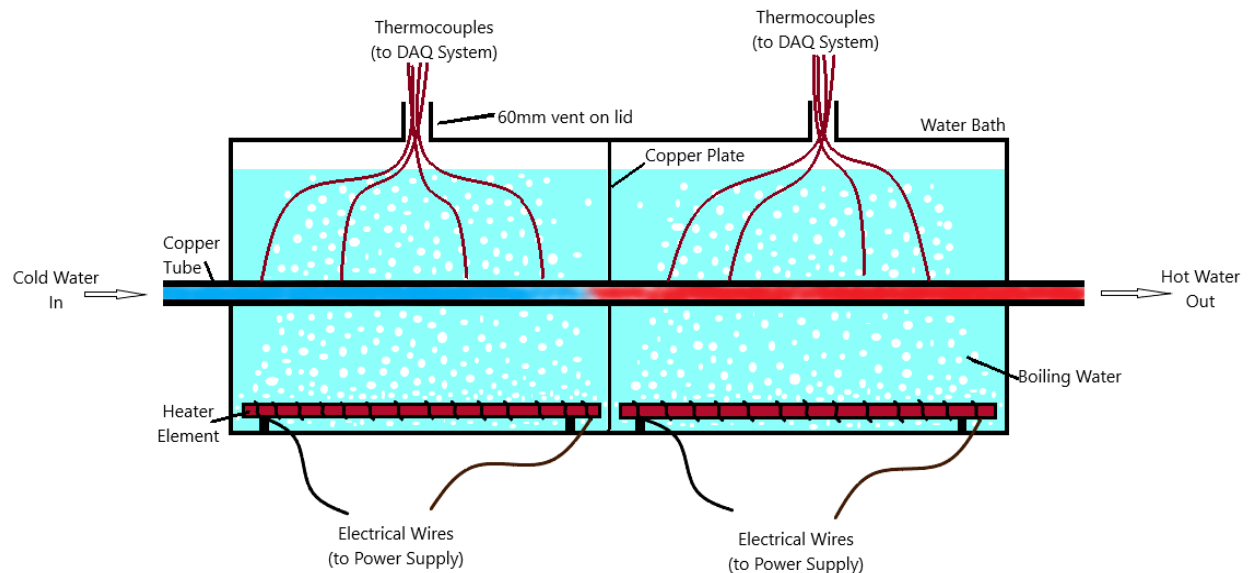
Fig. 3.2: Schematic of the water bath used to obtain a uniform surface temperature boundary condition, including the heater elements and test section.

The water inside the water bath was boiled using heater elements made of Constantan wire, which was tightly wound around a rectangular frame. To ensure uniform nucleate pool boiling, the frame of the heater elements covered the entire base surface area of each compartment. A small current through the heating wire was desired to prevent burnout, thus EA Elektro-Automatik bench power supplies with high voltage and low direct current output were used. The maximum power output of the power supplies was 3 kW, with a maximum voltage of 360 V and maximum current of 15

A. The electrical power input to the heater elements was manually controlled by adjusting the voltage and current input to the desired levels.

3.4. Test section

To measure the surface temperatures along the tube length, 24 T-type thermocouples were attached to the test section at eight stations (A-H), as shown in Fig 3.3. At each station, three thermocouples were carefully soldered onto the test section in a 0.3 mm indentation at radial angles of 120° to each other. To accurately measure the surface temperatures and avoid that the surface temperature measurements were biased to the boiling water inside the water bath, the thermocouple junctions were covered with a layer of epoxy (Araldite 2014-2) with a thermal conductivity of 0.035 W/mK, as shown in Fig. 3.4. The inlet and outlet temperatures of the fluid flowing through the test section were measured by two Pt100 probes.
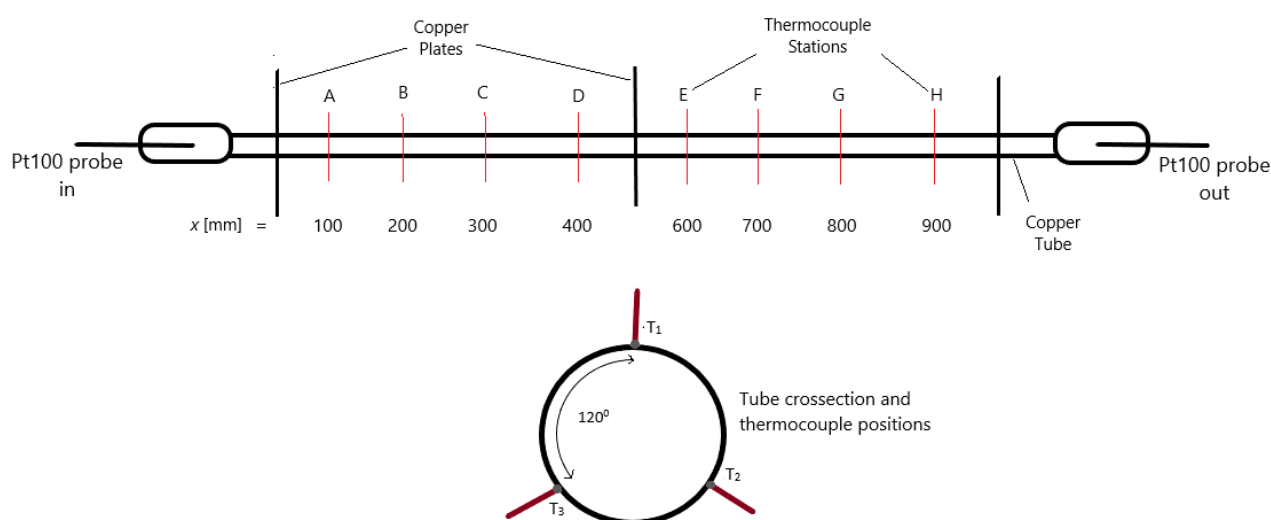
Fig. 3.3: Schematic of the test section indicating axial positions of the thermocouple stations as well as the circumferential placement of the thermocouples at each thermocouple station.
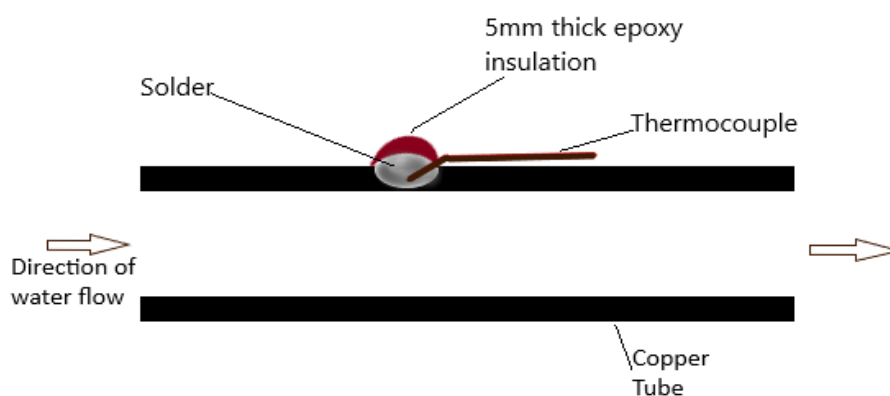
Fig. 3.4: Schematic representation of a thermocouple soldered to the test section and the junction covered with epoxy for thermal insulation

3.5. Experimental procedure and test matrix

Steady state conditions were deemed to have been reached when there was minimum deviation in the measurements of the mass flow rate, the inlet temperature, as well as the temperature of the boiling water inside the water bath. After the initial start of the system, approximately 120 minutes

15

were required to reach steady-state conditions of the whole system (inlet temperature, flow rate, power input and an even boiling).

For any set of tests done, the inlet temperature had to be set to a specific temperature. Water was pumped through the system using a positive displacement pump and a thermostat-controlled bath installed upstream of the tube's inlet kept the inlet tempreture to desired levels. Once the pump was switched on, the flow rate had to be maintained to a set point that corresponded to the desired Reynolds number. This was achieved using variable speed drives connected to the pump and also by adjusting the bypass and supply valves until a correct flow meter reading was recorded. Due to the low flow rates in laminar flow, the bypass valve was adjusted to increase backpressure on the pump for its optimal operation while the accumulator was kept operational to dampen the flow from any pulsations that would occur. The power supply that heated the heater elements inside the water bath was then switched on to the required levels by adjusting the voltage and current input.

Once steady state conditions were obtained, a total of 200 data points at 10 Hz were logged and averaged to produce a single experimental measurement for the temperatures and flow rate. Readings for the temperatures [°C], mass flow rate [mA converted to m^3s], Voltage [V] and Current [I] were all taken simultaneously for the respective tests completed. After a measurement was taken, approximately 30 minutes were required to reach steady state once one of the variables was changed, especially in cases where evaporated water had to be topped up inside the water bath or changes that required adjusting the flow rate. No values were recorded until all parameters were operating at the desired set points.

Experiments were conducted for Reynolds numbers between 500 and 3000 in order to sufficiently cover the laminar region of flow. Water inlet temperatures were varied between 20 °C and 80 °C. at 20 °C increments. The power input levels were adjusted accordingly between 1.5 kW and 7.5 kW for the different tests. The flow regime maps of Metais and Eckert [21] were employed to determine whether mixed or forced convection conditions dominated. With Ra = 2.9 x 10^6, Pr = 4.35 and Re = 500 at the lower Reynolds number limit and Ra = 2.1 x 10^6, Pr = 5.80 and Re = 3 000 at the upper limit, the flow was taken to be under mixed convection conditions for all tests.

The some of the most authoritative texts on heat transfer [5, 7, 42] suggest Eq. (3.1) to calculate thermal entry length of the tube.

$$L_{t,laminar} = 0.05 PrReD \tag{3.1}$$

Using this equation, the thermal entrance length of the test section at Re = 500 (the lowest considered Reynolds number) was found to be 0.98 m and greater than 4 m for Re = 2300. It was thus concluded that all tests on the 1 m-long test section employed, and the results begotten from experimentation were for thermally developing laminar flow, except for tests of Re = 500 where flow was just fully developed at the outlet. Everts and Meyer [20, 41] who have made the most recent developments on forced and mixed convection proposed Eq. (3.2) for mixed convection thermal entry lengths from their experiments with the uniform heat flux boundary condition:

$$L_{t,MC} = 0.12 RePrD \left(1 - \frac{Gr^{0.11}}{Pr^{0.5}Re^{0.07}} \right) \tag{3.2}$$

Using and Eq. (3.2), the thermal entrance length at the lowest Reynolds number was calculated to be greater than 8 m further supporting that flow was thermally developing for the bulk of the

16

experiments considered. The hydrodynamical length of the test section was longer than the thermal entrance lengths thus flow was assumed to be hydrodynamically developing as well.

3.6.   Calibration

The calibration methods detailed by Everts and Meyer [41] were followed whereby the Pt100 probes were calibrated to an accuracy of 0.06 °C using a DigiCal thermometer with an accuracy of 0.03 °C by placing them inside the thermostat-controlled bath. To eliminate the effects of change in properties at the junctions during soldering, the thermocouples along the test section were calibrated in situ to an accuracy of 0.1 °C using the calibrated Pt100 probes' measurements. During the thermocouple calibration, the whole test section was insulated using 120 mm thick Armaflex Class 0 insulation. Water from the thermostat-controlled bath was circulated through the test section at different temperatures and no heating was applied from the water bath. A single thermocouple was suspended inside the water bath at each thermocouple station to monitor the temperature of the boiling water during experimentation. These thermocouples were calibrated in situ using the thermostat-controlled bath and the Pt100 probes to measure the reference temperature. More details on the calibration steps taken are found in Appendix A.

3.7.   Data reduction method

The bulk fluid temperature for a tube length (x_1 - x_2) was determined from:

$$T_b = \frac{T_{in} + T_{out}}{2}$$

(3.3)

The fluid properties such as the specific heat, c_p, thermal conductivity, k, and the Prandtl number, Pr, were evaluated at the bulk fluid temperature across the specified length (x_1 - x_2) of the test section. For the full length of the tube, the inlet and outlet temperatures were measured using Pt100 probes at the inlet and outlet of the test section.

It was asserted that For a uniform surface temperature boundary condition, the LMTD methodology gives accurate values of the temperature difference between the bulk fluid and the inner surface of the test section, with a true reflection of how the local temperature difference decays exponentially [5]. This temperature difference was calculated using Eq. (3.4).

$$\Delta T_{lm} = \frac{T_{out} - T_{in}}{ln[(T_s - T_{out})/(T_s - T_{in})]}$$

(3.4)

The rate of heat transfer of the water inside the water bath could then be calculated as:

$$\dot{Q}_i = \dot{m}c_p(T_{out} - T_{in}) = h_i A_s \Delta T_{lm}$$

(3.5)

where A_s was the wetted surface area and h_i was the heat transfer coefficient of the water flowing through the test section. The heat transfer coefficient of water, h_i, obtained from the second part of Eq. (3.5) could then be used to calculate the Nusselt number inside the test section:

$$Nu = \frac{h_i D}{k}$$

(3.6)

where k was the thermal conductivity of the water flowing through the test section.

The various temperatures, heat transfer coefficients and thermal resistances involved in the system, at a given point *x* along the length of the test section, are illustrated in Fig. 3.5. Among other factors discussed in the results analysis, the representative thermal resistances (R_1, R_2, $R_{surface}$ and R_3) were taken to be accountable for the temperature differences and temperature gradients observed during testing.
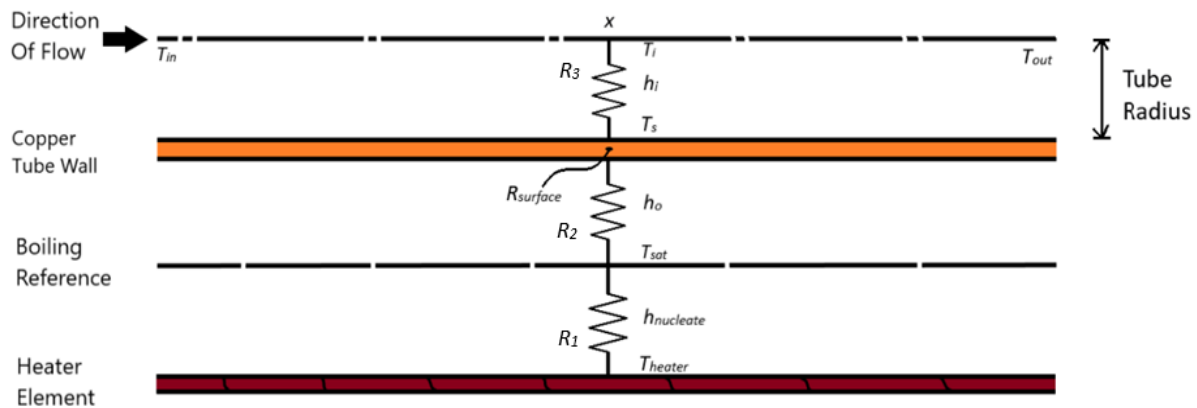
Fig. 3.5: Schematic of temperatures, heat transfer coefficients and thermal resistances prevalent in the system

To account for the thermal resistance of the copper test section, Eq. (3.7) was employed:

$$R_{surface} = \frac{ln\left(\frac{D_o}{D}\right)}{2\pi k_{Cu} L_{hx}}$$

(3.7)

where L_{hx} was the heated tube length and k_{Cu} the thermal conductivity of the copper tube. As the rate of heat transfer and thermal resistance of copper tube were known, the temperature differences across the tube wall could be calculated as:

$$\Delta T_{surface} = \dot{Q}_i R_{surface}$$

(3.8)

The temperature difference across the tube wall was less than 0.05 °C, which was lower than the uncertainty of the thermocouple measurements (0.1 °C). Therefore, it was concluded that temperature difference across the tube wall was negligible, and the thermocouples attached to the test section effectively measured the wetted surface temperature on the inside of the test section.
As the thermal resistance of the copper test section was negligible, an energy balance was applicable such that the average heat flux from the boiling water on the outside of the test section could be calculated from Eq. (3.9) [5]:

$$\dot{q}_o = \frac{\dot{Q}_i}{\pi D_o L} = h_o (T_{sat} - T_{s,ave})$$

(3.9)

Since the heater elements covered the full base of the water, providing an even distribution of heat, the heat transfer coefficient on the outside of the test section was expected to remain uniform along the full length of the test section. This would remain true unless there was a change in the heat input into the system.

The electric power supplied to an individual heater element was determined using:

18

$$Q_e = VI \tag{3.10}$$

Short electric cables from the 3 kW EA Elektro-Automatik bench power supplies to the heater elements were employed to minimise electrical resistances and heat losses. It was thus assumed that electric power input was essentially equal to the heat energy input into the system. The effects of changing the heat input on the surface temperature uniformity and the system as whole could thus be analysed. When more than one power supply was used, a sum of the individual products of voltage and current from each power supply was taken as the total power input.

The boiling regime prevalent in the water bath during experimentation was nucleate boiling. This boiling regime was governed by the boundary condition $5\,°C \leq \Delta T_{excess} \leq 30\,°C$, where ΔT_{excess} was the temperature difference between the heater elements surface (T_{heater}) and the saturation temperature (T_{sat}) of the boiling water [5]. The nucleate boiling heat flux could be determined using Eq. (3.11) developed by Rohsenow [43] where the properties of water were evaluated at the saturation temperatures.

$$\dot{q}_{nucleate} = \mu_l h_{fg} \left[\frac{g(\rho_l - \rho_v)}{\sigma} \right]^{1/2} \left[\frac{c_{p,l}\Delta T_{excess}}{C_{sf} h_{fg} Pr_l^n} \right]^3 = h_{nucleate}(T_{heater} - T_{sat}) \tag{3.11}$$

The heat transfer coefficient between the heater elements and the boiling water, $h_{nucleate}$, could be calculated from the Eq. (3.11) as well. This made it possible to determine the effects of changing the heat input on the different heat transfer coefficients in the system, h_i, h_o and $h_{nucleate}$.

The Reynolds number was calculated as:

$$Re = \frac{\rho v D}{\mu} \tag{2.1}$$

where the fluid density, ρ, and dynamic viscosity, μ, were evaluated at the bulk mean fluid temperature across the heated length of the test section.

3.8.   Uncertainty analysis

To increase reliability and instil confidence in the results, an uncertainty analysis was done for the measurements from the different instruments employed and the different heat transfer parameters. For the instrumentation, the suppliers' specified accuracies were considered during analysis. However, to avoid any distortions that would occur when soldering the thermocouples to the test section, they were calibrated using Pt100 probes to an uncertainty less than 0.1 °C. Everts and Meyer's [41] detailed procedures for calculating uncertainties of the heat transfer area, heat input, Reynolds numbers and Nusselt numbers within a 95% confidence interval were followed.

The Reynolds number uncertainty relied on the diameter of the tube, the dynamic viscosity and cross-sectional area. As presented in Appendix B, when the Reynolds number was increased, its uncertainty increased from approximately 2.2% to 2.6%. The average Nusselt number uncertainties were approximately 2% and decreased with an increase in the mass flow rates due to the small temperature difference between the surface of the test section and the bulk fluid. Increasing the inlet temperature also led to a slight decrease in the Nusselt number uncertainties, while the uncertainties increased up to 7% with increasing electrical input. This was due to the increased temperature gradients along the

tube length. For the same reason the heat transfer coefficients uncertainties also decreased with an increase in tube inlet temperature since the bulk fluid temperature were closer to the surface temperatures.

3.9.   Conclusions

This chapter focused on the experimental setup, data reduction method and experimental procedure. The test section was made up of a 1m long hard drawn copper tube immersed in boiling water in a water bath made up of two compartments. The compartments allowed for tests to be taken at both 1 m and 0.5 m lengths of the test section. The whole facility was sufficiently insulated to limit heat losses. The test facility employed, instrumentation and the recording of data were also discussed. The calibration methods for the thermocouples attached to the test section and the Pt100 probes were required to increase accuracy and reliability of measurements.

The Log Mean Temperature Difference was established as the best data reduction methodology for heat transfer experimentation with a uniform surface temperature thermal boundary condition. The data reduction method was reported in detail and an overview of the results of the uncertainty analysis is also presented. The Reynolds number uncertainties were only up to ±2.8%, while the Nusselt number uncertainties were less than 10%. Finally, the experimental procedures and test matrix were presented to detail the steps taken in experimentation and the extent of the tests completed.

4. VALIDATION

4.1. Introduction

In this chapter the experimental setup employed, and the data reduction methodologies are validated by comparing to correlations and heat transfer theories in literature on laminar flow with a uniform surface temperature boundary condition. This is to ascertain the reliability of the results from the experimental works. The theoretical bulk water temperature development and measurements were validated first, followed by the heat transfer coefficients in terms of the laminar Nusselt numbers.

4.2. Development of water temperatures along the test section

Correlations in literature for laminar flow under a uniform surface temperature boundary condition and the LMTD methodology were used as the guiding principles for the thermal analysis [5, 9, 10, 12-14]. A theoretical analysis was performed to predict the mean water temperatures at different axial positions along the test section, $T_{i,x}$. The predicted values at the test section's inlet, midsection and outlet were validated against the actual measurements at a Reynolds number of 1 300. The trend of the mean fluid temperatures along the tube could also be validated against findings in literature.

The heat transfer coefficients inside the test section, $h_{i,x}$, were computed from the Nusselt number equations summarised in Table 1. The limiting conditions of the different correlations were carefully considered and accounted for during the thermal analysis. The resultant mean fluid temperatures, $T_{i,x}$, could thus be obtained Eq. (3.5) expressed in differential form by Yousef and Tarasuk [15] as:

$$h_{i,x} = \frac{\dot{m} c_p}{\pi D} \cdot \frac{dT_b}{d_x} \cdot \frac{1}{T_s - T_b} \qquad (4.1)$$

Eq. (4.1) could also be expanded to:

$$h_{i,x} = \frac{\dot{m} c_p}{\pi D} \cdot \left(\frac{T_{i,2} - T_{i,1}}{x_2 - x_1} \right) \cdot \frac{1}{\left[(T_s - T_{i,1}) + (T_s - T_{i,2}) \right]/2} \qquad (4.2)$$

where (x_1 - x_2) was the distance between two successive thermocouple stations.

The results from the analysis were as presented in Fig. 4.1. The red and green markers represent the saturation temperature of the boiling water (T_{sat}) and the measured surface temperatures (T_s) along the tube length, respectively. The magenta and orange markers represent the measured inlet and outlet water temperatures (T_{in} and T_{out}), respectively, while the measured water temperatures at x = 0.5 m ($T_{i, 0.5}$) are represented using black markers. The blue lines represent the mean fluid temperature temperatures ($T_{i,x}$) obtained from Nusselt number correlations in literature. The predicted mean fluid temperature at x = 0.5 m was specifically compared to the measured value of $T_{i,0.5}$ = 60.50 °C.
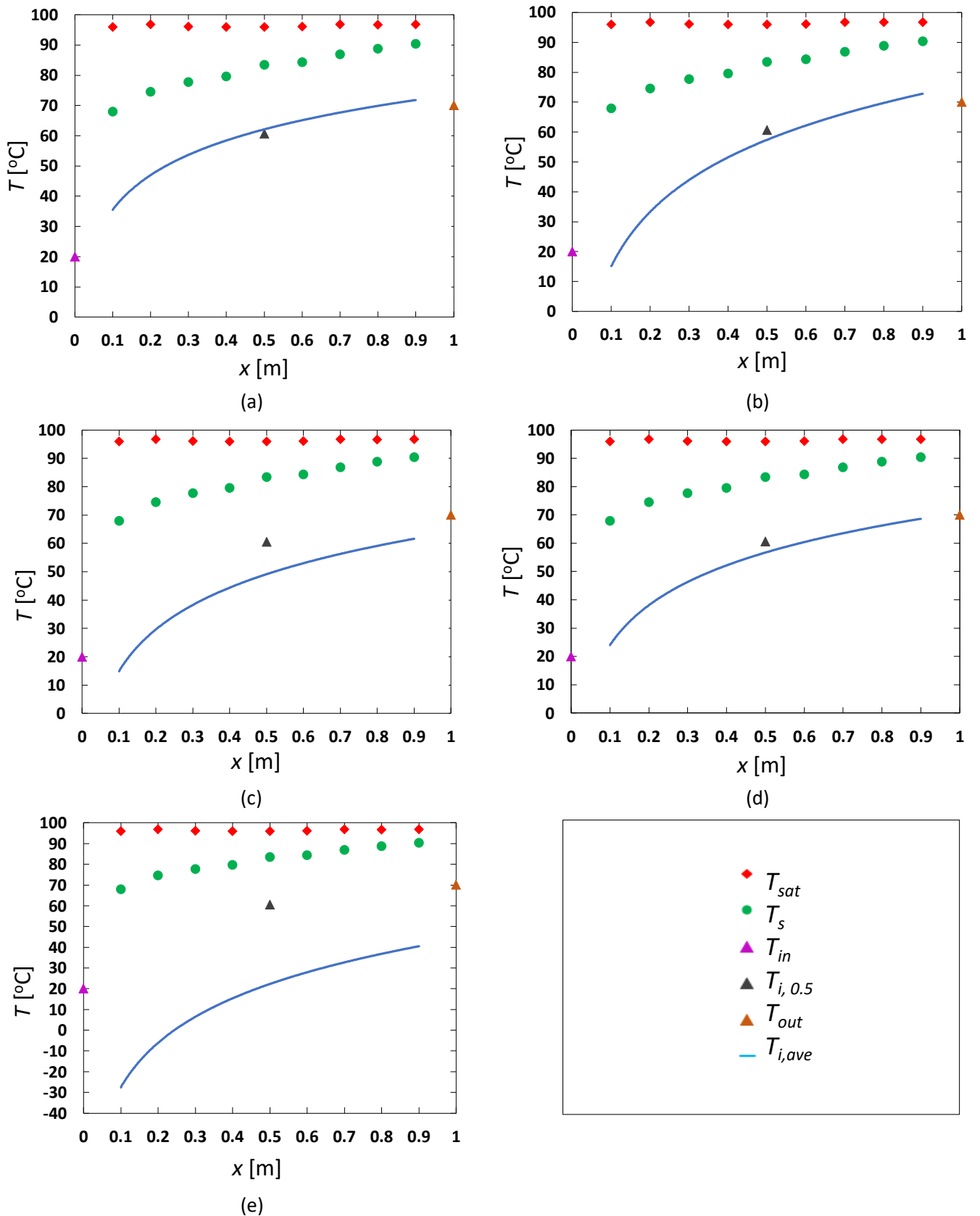
Fig. 4.1: Comparison of the measured saturation (red), inlet (magenta), outlet (orange) and mean fluid temperatures (black) at a Reynolds number of 1 300 with correlations in literature (solid blue line). The blue curves represent the predicted mean fluid temperature profiles across the tube ($T_{i,ave}$) using correlations of (a) Browns and Thomas [13], (b) Oliver [12], (c) Depew and August [14] (d) Colburn [9], (e) Sieder and Tate [10].

22

The mean fluid temperatures predicted using the correlations of Browns and Thomas [13] and Oliver [12] were within 1% of the measured fluid temperature at $x = 0.5$ m, validating the findings well. Colburn's correlation [9] yielded results with an 8.5% deviation and the remainder of the correlations had deviations greater than 10%. Yousef and Tarasuk [15] also noted a deviation of greater than 10% when they compared their experimental data with the results of Depew and August [13] who used ethyl alcohol as the test fluid. Furthermore, it should be noted that Depew and August [13] considered flow that was hydrodynamically fully developed at the onset of heating and forced convection was dominant. The mean fluid temperatures were significantly underpredicted when using the correlation of Sieder and Tate [10]. Eubank and Proctor [23] highlighted that the correlation of Sieder and Tate was limited only to $400 < \dot{m}c_p/kL < 700$ as it did not account for free convection effects, and was mainly applicable to viscous fluids such as oils or glycerine.

It follows from the blue curves in Fig. 4.1 that the mean fluid temperatures increased along the test section, approaching the surface temperatures. The expected logarithmic trend was not distinct, most probably due to the relatively short length of the test section and the flow being developing rather than becoming fully developed. However, Fig 4.1 showed trends typical of those predicted in literature (Fig 2.3 [5]), further increasing trust in the analyses.

Fig. 4.1 also showed that the measured surface temperatures along the test section were not uniform even though the saturation temperature of the boiling water remained constant. Although at different rates, it was observed that the difference between the saturation and the surface temperatures decayed in the same manner as the difference between the saturation temperature and the predicted mean fluid temperatures along the test section's length. This was well in agreement with Oliver [12], who asserted that convective movement would only start when some heat had been transferred from the surface to the fluid.

4.3.   Heat transfer coefficients

The LMTD method was employed to obtain the Nusselt numbers at $x = 0.5$ m and $x = 1$ m by considering three different values for the surface temperatures in Eq. (3.5). Fig. 4.2 compares the resultant Nusselt numbers with those from correlations in literature [9, 10, 12-15]. The cyan markers represent the Nusselt numbers obtained when considering the average surface temperatures, $T_{s,ave}$, measured by thermocouples along a length x. The green markers represent the Nusselt numbers obtained from the measured surface temperatures every 100 mm along the test section ($T_{s,x}$). Values for any points in between were extrapolated from the observed trend and used as needed. The red curve represents the Nusselt numbers obtained using the method of Colburn [9], where the saturation temperature was used as the surface temperature, $T_s = T_{s,sat}$.

It follows from Fig. 4.2 that at $x = 0.5$ m, the experimental Nusselt numbers assuming $T_s = T_{s,sat}$ were well within 3.3% of the value predicted by the Colburn correlation. For $T_s = T_{s,x}$ the experimental Nusselt numbers at $x = 0.5$ m were within 8% of the correlation developed by Brown and Thomas [13]. The slightly lower predicted Nusselt number was due to their use of a fully developed velocity profile at the onset of heating. It should also be noted that Brown and Thomas' correlation was based on the arithmetic mean temperature difference and not the LMTD. Fig. 4.2 also indicates that the experimental Nusselt numbers at $x =1$ m were within 5.3% of the correlations of Oliver [12], Depew and August [14], and Colburn [9] when the surface temperature was taken as either $T_{s,sat}$ and $T_{s,x}$. The surface temperatures measured by the thermocouples attached to the test section increased notably along the tube length. Thus when the assumption $T_s = T_{s,ave}$ was made in the LMTD calculations, the resultant Nusselt number values were inconsistent when compared to values from the correlations for both $x = 0.5$ m and $x = 1$ m. It is accepted in literature [5, 15] that the heat transfer process

23

observed along the test section is essentially self-diminishing due to the bulk fluid temperature approaching the fluid's surface temperatures as shown in Fig. 4.2. The Nusselt numbers were greater at 0.5 m than at 1 m and was expected to approach a constant value if the flow had become fully developed, as predicted by other researchers [15, 20, 34].
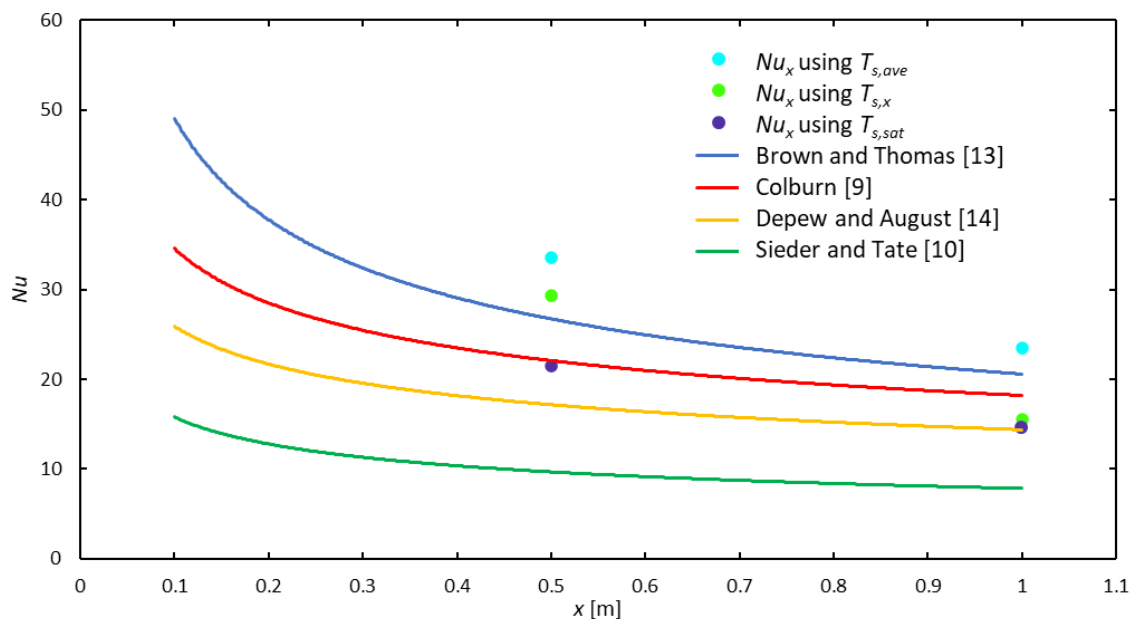

Fig. 4.2: Comparison of the Nusselt numbers at x = 0.5 m and x = 1 m calculated using the LMTD method and three different considerations of values to use as the surface temperature ($T_{s,ave}$, $T_{s,x}$, $T_{s,sat}$) with local Nusselt number correlations in literature [9, 10, 13, 14].

4.4.   Conclusions

The experimental set up's temperature measurements were validated as well as the heat transfer coefficients for laminar flow. The bulk water temperatures measured at 0.5 m of the test section corelated within 1% of at least two of the correlations found in literature on laminar flow under a uniform surface temperature boundary condition. It was also observed that the difference between the saturation and the surface temperatures decayed in the same manner as the difference between the saturation and the predicted fluid temperatures along the test section's length, though it was at different rates. The development of the predicted mean water temperatures was as is predicted in some of the most authoritative texts in heat exchange. However, further investigations into the phenomenon are still needed especially with longer test section lengths. The heat transfer coefficients calculated using the LMTD Methodology were validated against those predicted using various correlations from relevant texts found in literature. These too correlated well with literature and the reasons for any variations were due to the different experimental set ups and conditions used in developing the correlations.

24

5. RESULTS

5.1. Introduction

This chapter presents the results from direct observations during experimentation and calculations during the data analysis. The main objectives of the study determined the scope of works and hence guided the thermal analyses in order to obtain the required information. The observed trends of the surface temperatures across the test section during experiments are first detailed. The effects of changing different experimental parameters on the uniformity of the surface temperatures follow. These include changes in Reynolds Numbers (within the laminar flow regime), the inlet temperatures, and the heat input into the system. An analysis on the conditions needed to maintain a uniform surface temperature for developing laminar flow across a horizontal test section immersed in water boiling at a constant temperature is detailed in the last section, leading to the scientific conclusions.

5.2. Surface temperature measurements

To obtain a uniform surface temperature boundary condition of the test section, nucleate pool boiling was used. Although the saturation temperature of the boiling water was uniform, the recorded surface temperatures on the inside of the test section were not, presenting a gradually increasing trend. Fig. 5.1 compares the measured surface temperatures along the test section with the saturation temperature of the water. The measured surface temperature showed a rising trend, approaching the constant saturation temperature asymptotically as the flow developed along the tube length. It was still expected to approach a constant value once the flow was fully developed. The increasing surface temperatures shown in Fig. 5.1 entailed that the thermal resistance between the boiling water and the water flowing through the test section decreased along the tube length. Further experimental investigations into the factors that would affect the surface temperature uniformity were thus necessary. This included the Reynolds number, the inlet temperatures, and the heat input to the boiling water.

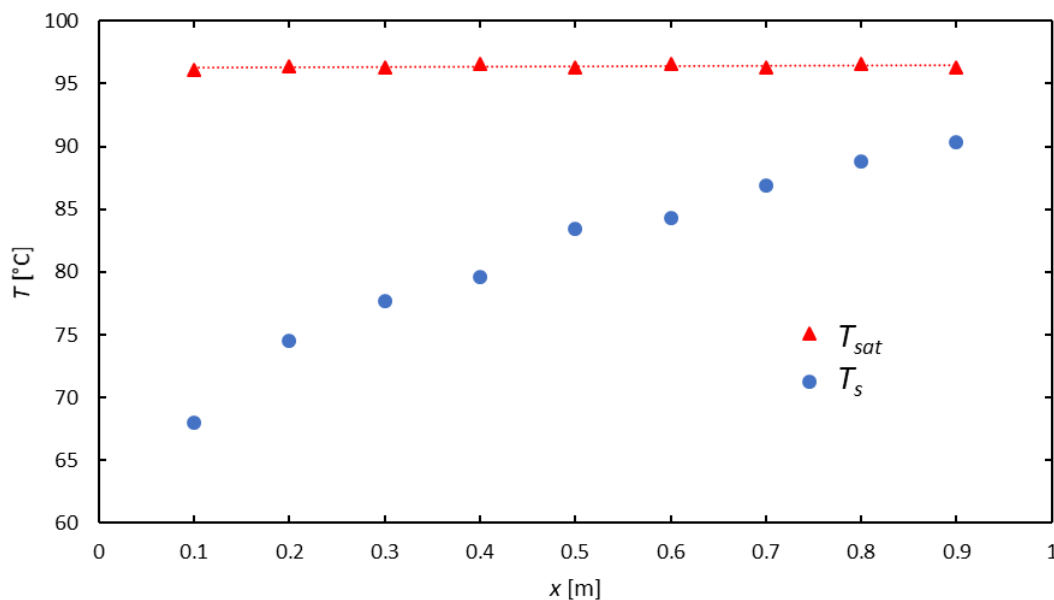Fig. 5.1: Comparison of the measured surface temperatures along the 1 m length and the saturation temperatures of the boiling water at a Reynolds number of 1 300.

5.3. Effect of Reynolds number on surface temperature uniformity

To investigate the effect of Reynolds number on the surface temperature uniformity, experiments were conducted using the full 1 m tube length at six different Reynolds numbers. The inlet

25

temperature was kept constant at 20 °C for all tests and the results are compared in Fig 5.2. For all Reynolds numbers considered, the surface temperatures generally increased along the test section. However, the degree of uniformity improved with increasing Reynolds numbers. The difference between the uniform saturation temperature, T_{sat}, and the measured wetted surface temperatures, T_s, decayed exponentially along the tube length for all the Reynolds numbers considered.
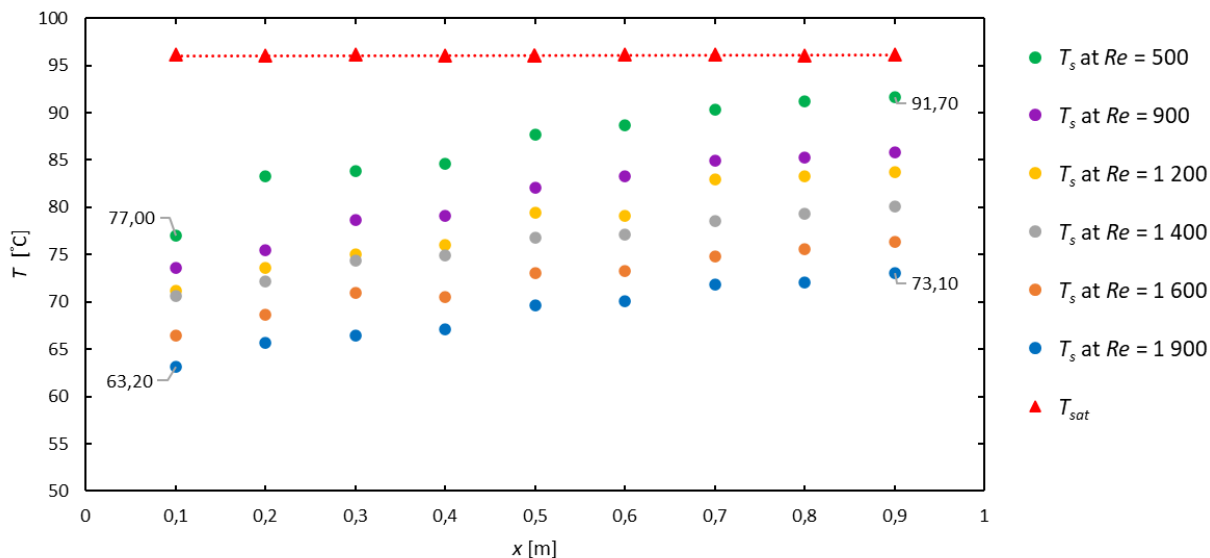
Fig. 5.2: Comparison of the saturation temperature of 96.5 °C with the surface temperatures along the test section at different Reynolds numbers.

To critically evaluate the surface temperature uniformity observed in Fig. 5.1, Fig. 5.3 was further developed. A comparison was made of the temperature difference between the inlet and outlet (red markers) with the difference between the average surface and bulk fluid temperatures (green markers), as well as the difference between the maximum and minimum surface temperatures (blue markers) for their respective Reynolds numbers.

Fig. 5.3: Comparison of the differences between the inlet and outlet temperatures, the maximum surface temperature and the outlet temperature, and maximum and minimum surface temperatures as a function of Reynolds number.

As expected from literature [5], the red markers in Fig. 5.3 indicated that the difference between the inlet and outlet temperatures decreased with increasing Reynolds number. Although the lower Reynolds numbers yielded surface temperatures closer to the saturation temperature, the blue markers in Fig. 5.4 indicated that the surface temperature difference across the test section, whic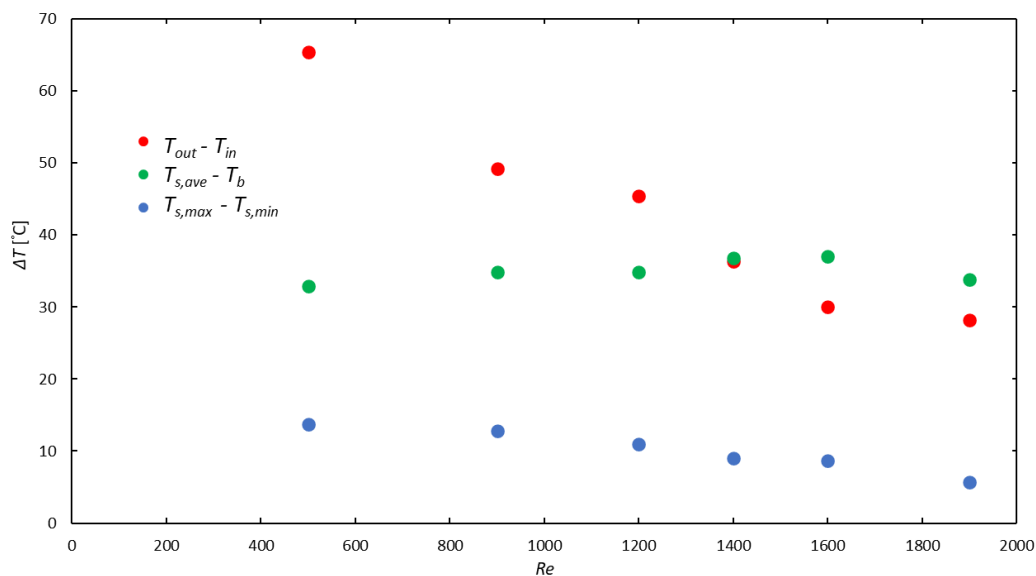h is an indication of the surface temperature uniformity, was greater for lower Reynolds numbers than at the higher Reynolds numbers. This therefore implied an improved surface temperature uniformity with increasing Reynolds number.

The influence of free convection is expected to increase as the difference between the surface temperature and the fluid temperature flowing through the test section increases [12, 15]. Although it is not prominent, it seems from the green markers in Fig. 5.3 that there was this slight increase with increasing Reynolds numbers. Free convection effects are generally expected to decrease with increasing Reynolds number as they are suppressed by the increased fluid velocity [37]. This temperature difference was therefore more likely to be due to developing flow, rather than mixed convection.

5.4.   Effect of inlet temperature on surface temperature uniformity

To investigate the effect of varying the inlet temperature on the surface temperature uniformity, five different inlet temperature values were considered. As established from Fig. 5.2 and 5.3, the highest degree of surface temperature uniformity in the laminar flow was at relatively higher Reynolds numbers. Therefore, a Reynolds number of 2 000 was maintained for all tests to increase chances of achieving surface temperature uniformity. However, for all the tests taken, there was no set of measurements where the surface temperatures were uniform as shown in Fig. 5.4. As the inlet temperature was increased, the average surface temperatures also increased. The surface temperature uniformity also improved with increase in tube inlet temperatures. This was due to the decreased surface-fluid temperature differences inside the test section and thus a reduced thermal resistance. However, it should be noted that the rate of heat transfer at these high inlet temperatures is very low due to the small surface-fluid temperature differences, which is not favoured in heat exchanger applications [44].
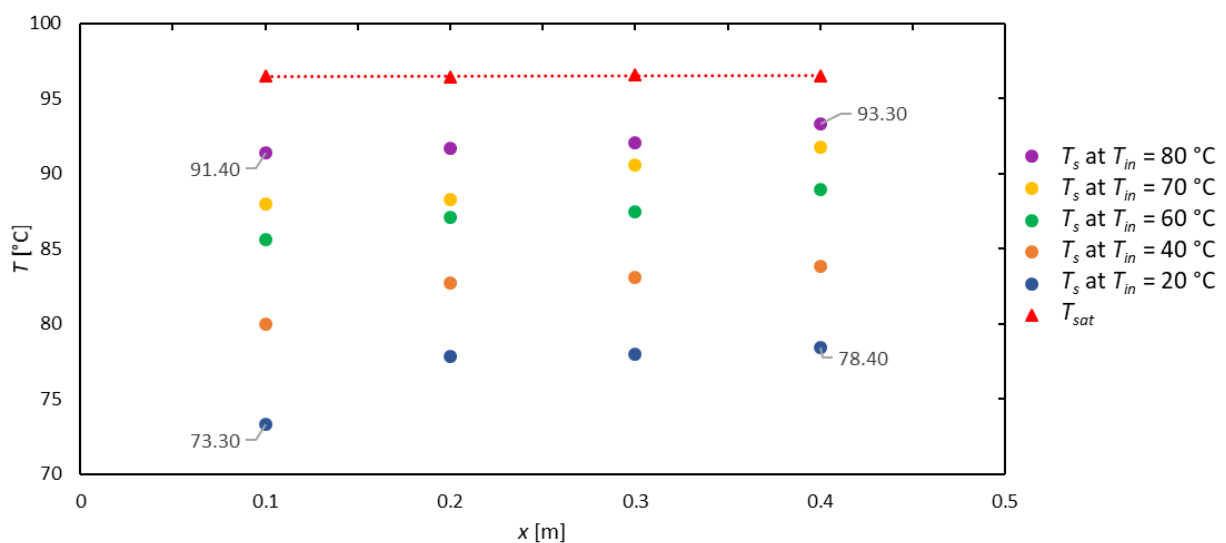

Fig. 5.4: Comparison of the surface temperatures (T_s) across a 0.5m length of the test section for different inlet temperatures (T_{in}) at a constant Reynolds number of 2 000

27

5.5. Effect of heat input on surface temperature uniformity

While keeping the inlet temperature fixed at 20 ˚C, the effect of varying the heat input (from the power supplies) to the water bath on the surface temperature uniformity was investigated. Experiments were conducted and controlled at about a median value of the laminar Reynolds number range. For all the different levels of heat input into the system considered, the Reynolds number was thus maintained at 1 300. Increasing the heat input would increase the heat flux to the boiling water which in turn would increase the heat transfer rate between the boiling water and the water flowing through the test section. Fig. 5.5 compares the surface temperatures along the test section for the different heat input levels across a 0.5 m length of the test section.
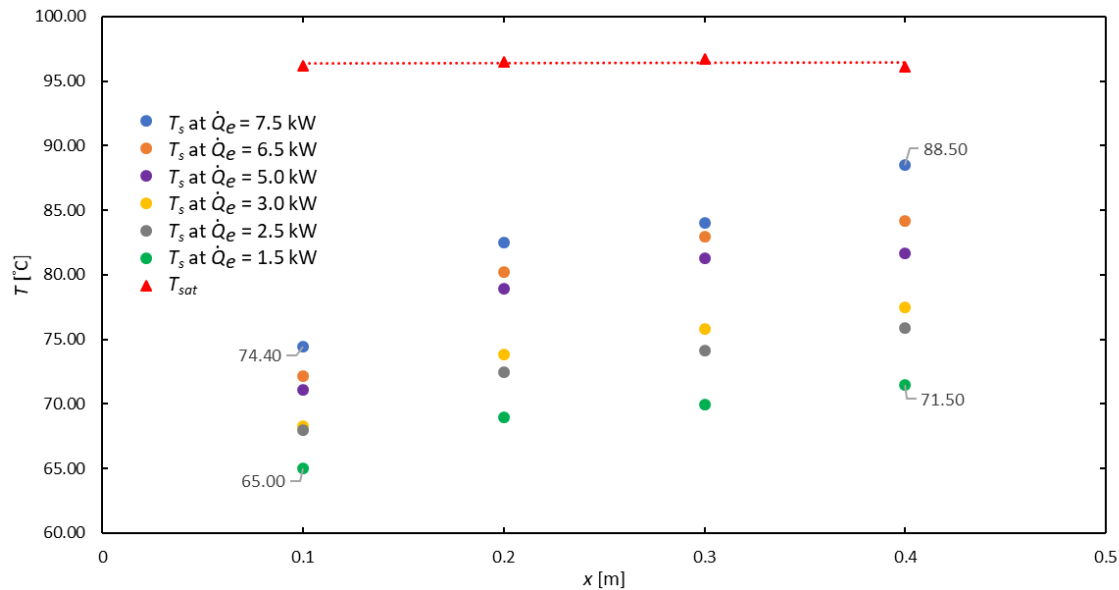

Fig. 5.5: Comparison of the measured surface and saturation temperatures along the test section for different heat inputs at a fixed Reynolds number of 1 300

An increased heat input resulted in increased average surface temperatures, while there was no notable change in the measured saturation temperatures of the water in the water bath. However, an increased heat input also led to increased non-uniformity of the surface temperatures along the test section. This was shown in the differences between the maximum and minimum measured surface temperatures labelled in Fig. 5.5 for the maximum and minimum heat inputs, respectively. It should be noted that changing the heat input affected the heat transfer characteristics of the whole system. Although not indicated in Fig. 5.5, an increased heat input also increased the outlet water temperature, which was as expected.

Fig. 5.6 compares the influence of heat input on the different heat transfer coefficients present in the system. As the heat input was increased, the average heat transfer coefficients between the heater element and the boiling water, $h_{nucleate}$, between the boiling water and the surface of the test section, h_o, and between the surface of the test section and the water flowing through it, h_i, increased. However, the rate of increase of h_i with increasing heat input was much lower than that for $h_{nucleate}$ and h_o, respectively. The h_i trend seemed to be approaching a constant value, indicating that a continuous increase in heat input to the boiling water could reach a limit in terms of beneficial heat transferred to the water flowing through the test section.
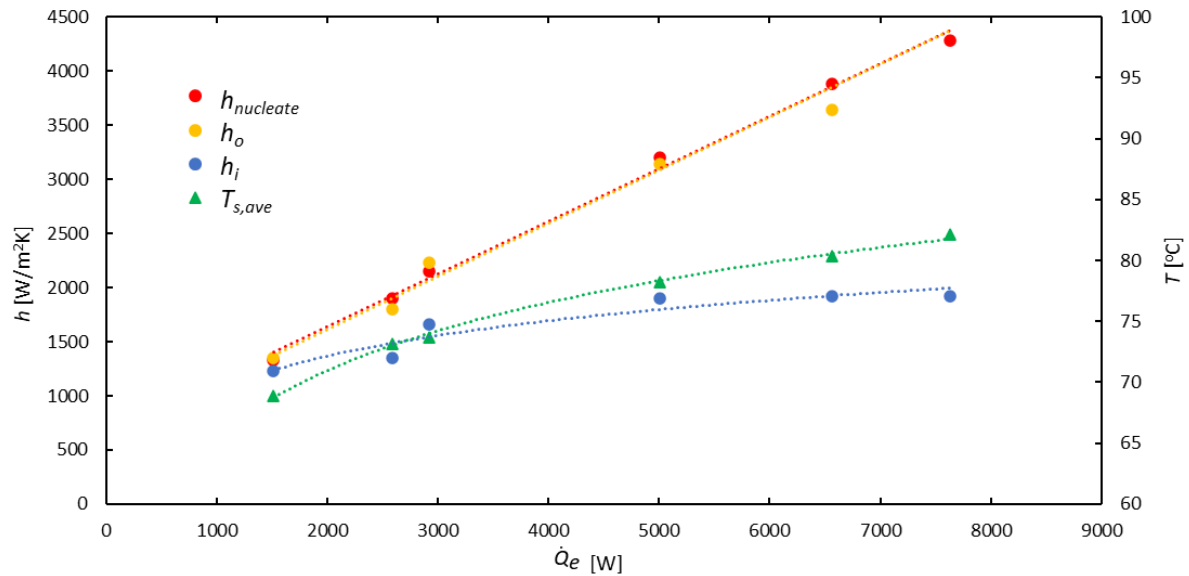
28

Fig. 5.6 Comparison of the heat transfer coefficients between the heater elements and boiling water ($h_{nucleate}$), between the boiling water and test section (h_o), and between the test section and water flowing through the test section (h_i) as a function of heat input ($\dot{Q}_e$).The average surface temperatures ($T_{s,ave}$) as a function of heat input are also given.

To gain a better understanding of the causes for the different trends of h_i and h_o in Fig. 5.6, Fig. 5.7 was used to compare the heat input (from the power supply) to the heat transfer to the water inside the test section and the heat losses as a function of heat input. This figure indicates that an increased heat input to the system resulted in continuously greater heat losses without any noteworthy increase in heat transfer to the water flowing through the test section. Increasing the heat input by a factor of 5 only increased the heat transferred to the water flowing through the test section by a factor of 1.66, while the heat losses increased by a factor of 8.28. The heat losses were mainly due the continuously increasing rate of evaporation which was observed as the heat input was increased.
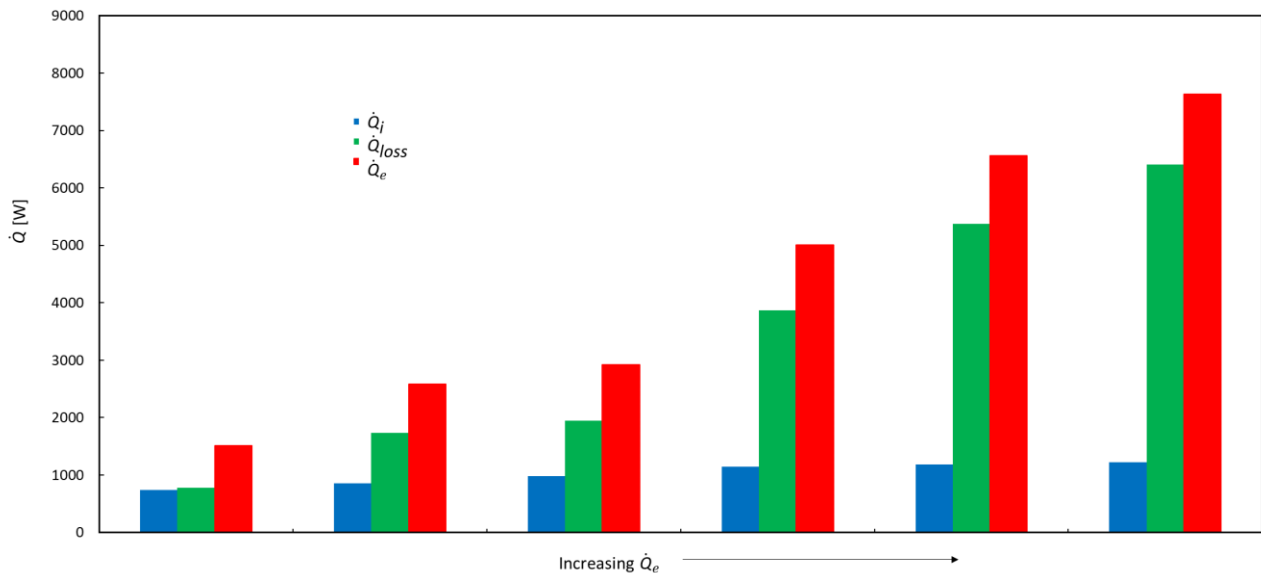
Fig. 5.7: Comparison of the heat input, $\dot{Q}_e$, heat transferred to water flowing through the test section, $\dot{Q}_i$ and heat losses, $\dot{Q}_{loss}$, as a function of the mentioned heat input, $\dot{Q}_e$, to the heater element.

Based on these experimental observations, a numerical analysis was done to estimate how much heat input would be needed to achieve uniform surface temperatures if the electrical power input was increased above 7.5 kW. Two conditions needed to be satisfied simultaneously. Firstly, the trends of

29

the average heat transfer coefficients inside the test section as a function of the outlet fluid temperature were plotted (as shown in Fig 5.8) for increasing electrical heat input from 1.5 kW to 7.5 kW. Both linear and logarithmic approximations were considered. The logarithmic approximation was motivated because the last three points approached a constant value. Thus, it was assumed that if the electrical input was increased, h_i and T_{out} would follow either of the two approximations when extrapolated.

Fig. 5.8: Comparison of the heat transfer coefficient inside the test section, h_i, as a function of the water outlet temperatures, T_{out}, for both linear and logarithmic trends for increasing electrical heat input.
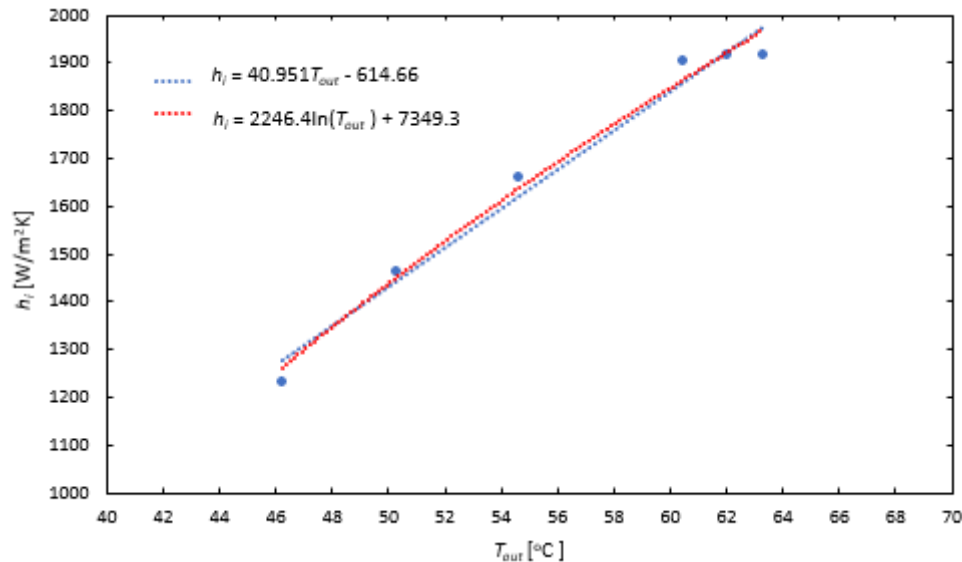
Secondly, it was assumed that the maximum uniform surface temperature achievable would be equal to the saturation temperature of the boiling water inside the water bath (T_{sat} = 96.50 °C). Using the LMTD methodology, the values of h_i and T_{out} that would satisfy T_s = 96.50 °C, as well as the respective correlations in Fig 5.8, were then determined by iteration. A fixed laminar Reynolds number of 1 300 and an inlet temperature of 20 °C were considered for this analysis. Once the maximum values of the outlet temperature, $T_{out,max}$, and heat transfer coefficients, $h_{i,max}$, were determined for both approximations, two values of the maximum rate of heat transfer to the tube, $\dot{Q}_{i,max}$, could then be estimated using Eq. (3.5).

The trends of the heat transfer rate to the water as a function of electrical input were then graphically investigated in Fig. 5.9. The respective linear and logarithmic approximated values of the maximum heat transfer rate are also indicated. From this graph it follows that to satisfy a uniform surface temperature boundary condition that corresponded to the saturation temperature of the boiling water, and assuming that the h_i, vs T_{out} data followed either a linear or logarithmic trend when heat was added into the system, heat inputs of 14.6 kW or 31.3 kW would be required. However, supplying such high power levels was not feasible compared to the size of the system and would not be desirable for practical applications. Furthermore, if data was to follow the trends in Fig 5.7 and Fig. 5.9, it would be energy inefficient to run such a system with potential heat losses of up to 12.8 kW for the linear approximation and 28.2 kW for the logarithmic approximation expected. It was thus concluded that the surface temperature could not be made uniform by increasing the electrical power input.
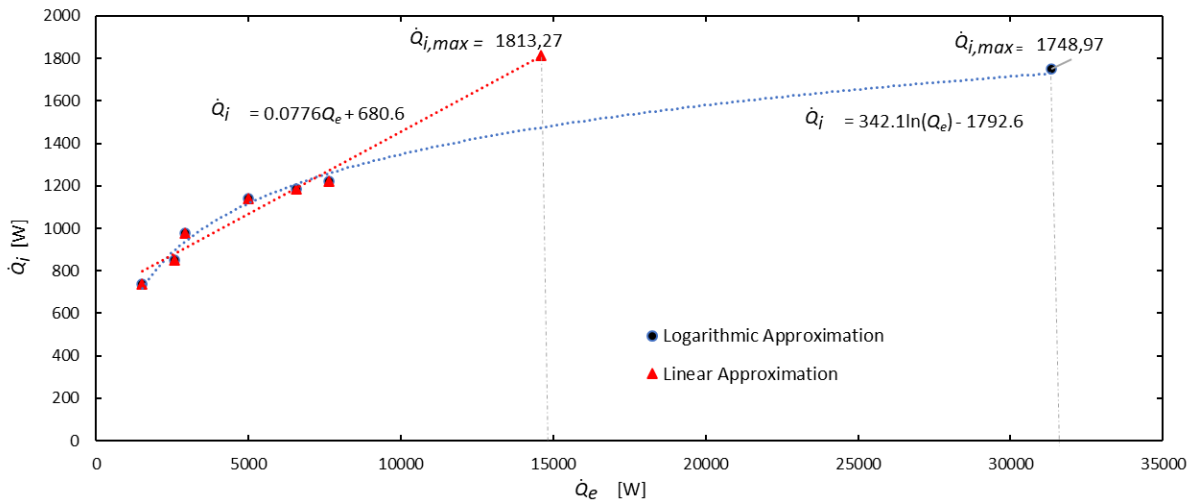
Fig. 5.9: Logarithmic and linear approximation of required electrical heat input to sustain surface temperatures equal to the saturation temperature $T_s = T_{sat} = 96.5$ °C

5.6. Effect of developing flow

It follows from Fig 5.1 that the surface temperatures increased along the tube length and approached the saturation temperature near the outlet of the test section. Fig. 5.2 further indicated that the surface temperature uniformity improved with increasing Reynolds number. This was attributed to the smaller temperature differences that exist at the inlet and outlet at higher flow rates. The surface temperatures measured at Reynolds numbers of 500 and 1 900 respectively are compared in Fig. 5.10.
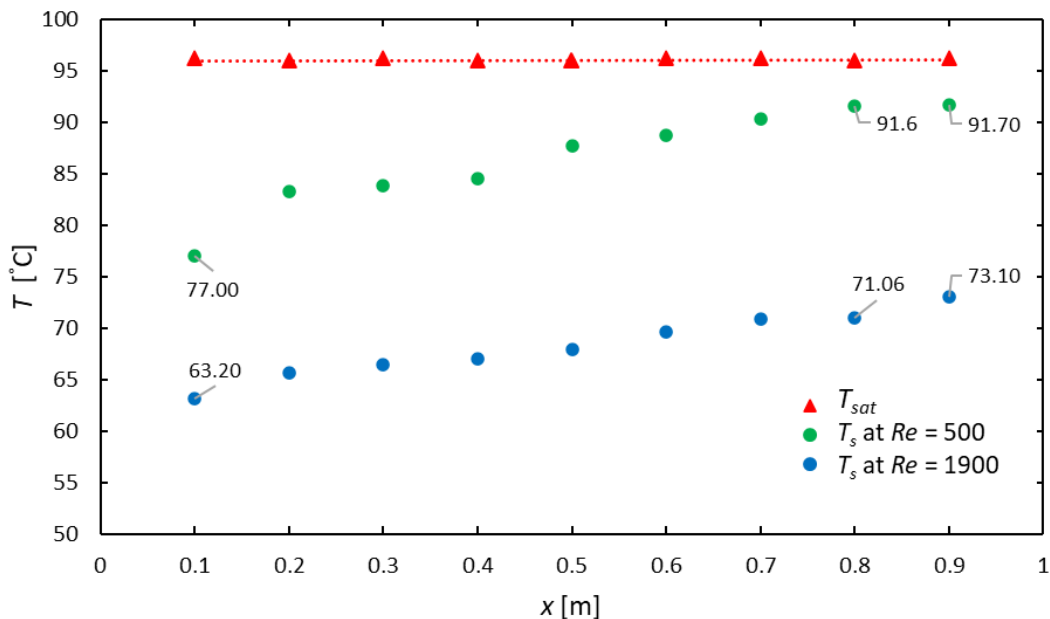
Fig. 5.10: Comparison of the saturation temperature of 96.5 °C with the surface temperatures along the test section at Reynolds numbers of 500 and 1 900.

From close inspection, it was observed that at the minimum Reynolds number of 500, the surface temperature became approximately constant at the last two thermocouple stations (as the flow became fully thermally developed), while they continued to increase along the tube length at a Reynolds number of 1 900 (where flow was still developing). The theoretical entrance lengths at Reynolds numbers of 500 and 1 900, as calculated from Eq. (3.1), were 0.98 m and 4.2 m, respectively.

31

Therefore, the main reason behind the increasing surface temperatures along the tube length, and thus the temperature nonuniformity, was most probably the fact that the flow through the test section was developing rather than fully developed. Although the test section length was not sufficient to obtain fully developed flow at higher Reynolds numbers, it was postulated that the surface temperatures would then remain constant for the fully developed lengths.
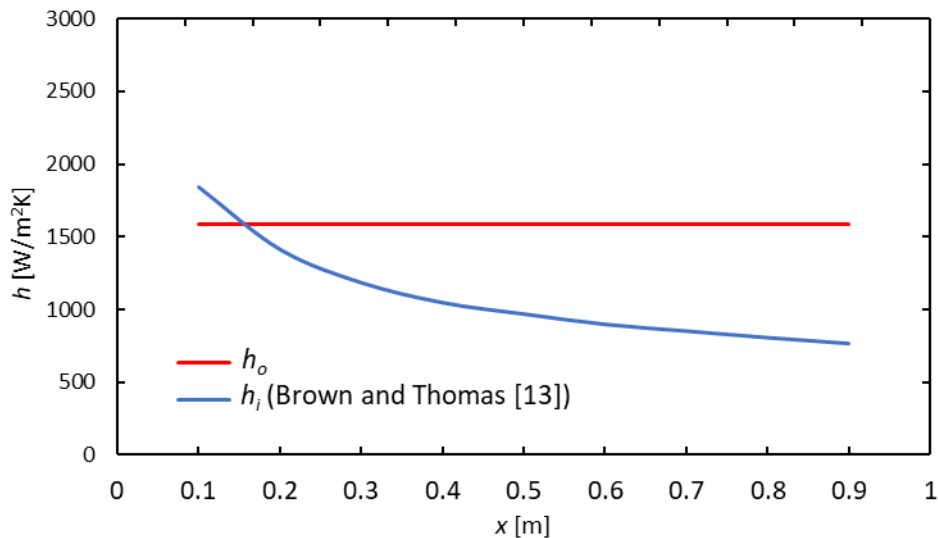
(a)
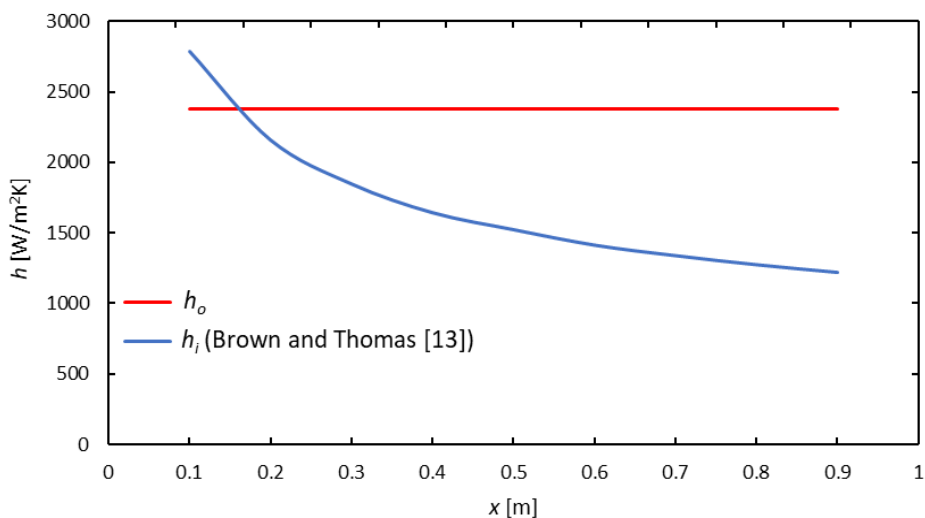
(b)

Fig. 5.11: Comparison of the internal flow heat transfer coefficients predicted using the Brown and Thomas correlation [13] and the heat transfer coefficients from the boiling water to the outside surface of the tube (h_o) at (a) Re = 500 and (b) Re = 1 900.

For developing flow, the maximum heat transfer coefficients are found near the inlet of the test section, and they gradually decrease along the length of the test section as the flow develops and become constant once the flow is fully developed [5, 18]. Fig. 5.11 compares the heat transfer coefficients on the inside of the test section, predicted using the correlation of Brown and Thomas [13], for Re = 500 and Re = 1 900 respectively as well as the boiling heat transfer coefficient on the outside of the test section. This figure indicates that, near the inlet of the test section, the heat transfer coefficients on the inside of the test section were higher than those on the outside of the test section. However, as the flow developed along the tube length, the outer heat transfer coefficients began to

32

dominate and the difference between the outer and inner heat transfer coefficients increased along the tube length. Furthermore, the difference between the heat transfer coefficients inside and outside the test section was greater for higher Reynolds numbers. When comparing the results in Fig. 5.10 and Fig. 5.11, it follows that the axial position at which the two heat transfer correlations crossed in Fig. 5.11, corresponded to a significant change in the gradient of the surface temperatures in Fig. 5.10. This confirms that the surface temperatures are affected by the interaction of the heat transfer coefficients inside and outside the test section.

As it was not possible to significantly increase the heat transfer coefficients on the outside of the test section by increasing the heat flux, the high heat transfer coefficients (due to developing flow) on the inside of the test section remained significant in comparison to the heat transfer coefficient outside the test section. This caused the surface temperature to increase instead of being uniform or equal to the saturation temperature of the boiling fluid. However, as the flow developed and the inner heat transfer coefficients decreased, the effects on the surface temperatures also decreased and thus they would approach a constant value as well. It was therefore concluded that the assumption of a uniform surface temperature for a test section subjected to phase-change on the outside is not valid for developing laminar flow. This was a valuable conclusion which had never been established in previous studies.

5.7. Conclusions

Although the boiling water in the water bath was at a constant temperature of saturation, the recorded surface temperatures on the inside surface of the immersed test section were not. Unexpectedly, the surface temperatures presented a gradually increasing trend. The temperature difference between the saturation temperature and the measured surface temperature decayed exponentially as the flow developed along the tube length and was expected to reach a constant once flow was fully developed. The effects of changing three critical parameters to the measured surface temperatures uniformity was further investigated.

For all Reynolds numbers considered, the surface temperatures generally increased along the test section. Although the lower Reynolds numbers yielded surface temperatures closer to the saturation temperature, observed trends indicated that the surface temperature difference across the test section was greater for lower Reynolds numbers than at the higher Reynolds numbers. Therefore, degree of uniformity improved with increasing Reynolds numbers. Increasing the inlet temperature also improved the degree of uniformity of the measured surface temperatures while the average surface temperatures increased as well. This was largely attributed to the decreased surface-fluid temperature differences inside the test section and thus a reduced thermal resistance. However, it should be noted that for all tests considered, none yielded sufficiently uniform surface temperatures.

Increasing heat input into the system resulted in increased average surface temperatures, while there was no notable change in the measured saturation temperatures of the water in the water bath. However, an increased heat input led to increased non-uniformity of the surface temperatures along the test section. It was also noted that changing the heat input affected the heat transfer characteristics of the whole system. As the heat input increased, the average heat transfer coefficients between the heater element and the boiling water, between the boiling water and the surface of the test section, and between the surface of the test section and the water flowing through it also increased. However, the rate of increase of the heat transfer between the surface of the test section and the water flowing through was much lower than that for the other two respectively and seemed to be approaching a constant value. This indicated that a continuous increase in heat input to the boiling water could reach a limit in terms of beneficial heat transferred to the water flowing through the test section.

33

Further analyses showed that an increased heat input to the system resulted in continuously greater heat losses through evaporation without any noteworthy increase in heat transfer to the water flowing through the test section. Increasing the heat input by a factor of 5 only increased the heat transferred to the water flowing through the test section by a factor of 1.66, while the heat losses undesirably doubled. It was concluded that it would be impractical to sustain such a system with very high energy input requirements due to the high energy losses from evaporation.

After comparing the developing heat transfer coefficients inside the test section with the boiling heat transfer coefficients outside the test section, it was concluded that the surface temperature uniformity was mainly due to the flow being developing rather than fully developed. The main reason behind the observed increasing surface temperatures was thus attributed to the high heat transfer coefficients in the entrance region. As the flow developed along the tube length, the heat transfer coefficients decreased and the boiling heat transfer coefficients outside the test section began to dominate. Thus, it was concluded that for flow through a horizontal test section immersed in boiling water, the surface temperatures will increase along the tube length and only approach a constant value when flow is fully developed.

6. SUMMARY, CONCLUSIONS AND RECOMMENDATIONS

6.1. Summary

Heat exchangers in which there is phase-change (boiling and condensation) on at least one side of the heat transfer surface are some of the most critical components of the thermodynamic cycles of many clean energy generation facilities, air conditioning systems and refrigeration cycles. Engineering designs for these are dependent on an understanding into the fundamentals of the thermal processes that occur when these systems are operational. Several experimental studies have been done on the uniform surface temperature boundary condition using a variety of experimental setups. However, from research into literature, very little is mentioned on the surface temperature non-uniformity during developing laminar flow, even though uniform surface temperature thermal boundary conditions would have been assumed due to the constant saturation temperature on one or the other side of the heat transfer surface.

The purpose of the study was thus to investigate the inner surface temperature uniformity for internal single-phase developing laminar flow through a horizontal tube exposed to nucleate pool boiling on the outer surface. The test section was made of smooth surfaced and hard drawn copper tube running through the centre of a water bath divided into two compartments. The test section had a length of 1 m and inner diameter of 11.2 mm. Nucleate boiling was brought about by means of heater elements that covered the entire base area of the water bath to ensure an even distribution of heat.

Specific focus was drawn to the development of the surface temperatures on the inside of the test section during simultaneously hydrodynamically and thermally developing flow of water. Experiments were conducted between Reynolds numbers of 450 and 3 000 and using different heat input levels and inlet temperatures. The experimental measurements were recorded and analysed using computer-based software. Thermal principles and correlations accepted in literature were used to validate the experiment, reduce the data and calculate parameters required in order to achieve set objectives. These included studies into the effects of Reynolds Number, tube inlet temperatures and the heat input on surface temperature uniformity.

6.2. Conclusions

A thermal analysis was done using the Log Mean Temperature Difference Method (LMTD) and fundamental heat exchange principles for a uniform surface temperature boundary condition. For comparison with the experimental findings, care was taken to establish the different experimental setups employed by previous studies, their scientific assumptions, and the data reduction techniques they used. The results were validated and agreed well with existing correlations in literature. However, it was observed that in the entrance region of laminar flow with a uniform temperature on the outside of the test section, the surface temperatures were not uniform. As had never been established in past literature, the measured surface temperatures exhibited a rising trend approaching a constant value that remained less than the saturation temperature.

Although it was found that the temperature uniformity improved with increasing Reynolds numbers, the temperature difference between the average surface and saturation temperatures increased due to the decreased mean fluid temperatures inside the test section. Furthermore, an increase in inlet temperatures also improved the surface temperature uniformity, but the very small surface-fluid temperature differences were not favourable for heat exchanger applications.

Increasing the heat input in turn increased the heat transfer coefficients, the fluid temperature measured at the outlet of the test section, as well as the surface temperatures. However, it also decreased the surface temperature uniformity. Increasing the heat input to the system did not significantly increase the heat transfer to the water flowing through the tube, as much of the heat added was lost through evaporation and miscellaneous losses. Further analysis showed that it would be impractical to make the surface temperatures uniform by means of increasing heat input. For the experimental setup designed, increasing the heat input by a factor of 5 only increased the heat transferred to the water flowing through the test section by a factor of 1.66, while the heat losses increased by a factor of 8.28.

It was found that the surface temperature uniformity was mainly due to the flow being developing rather than fully developed. The high heat transfer coefficients associated with developing flow were not dominated by the boiling heat transfer coefficients on the outside of the test section. However, as the flow developed along the tube length, the heat transfer coefficients decreased and the boiling heat transfer coefficients outside the test section began to dominate. Therefore, the general assumption of a uniform surface temperature boundary condition during phase-change conditions will only be valid for fully developed flow and is not valid when the flow is still developing.

6.3. Recommendations

To further this research:

- Experimentation with longer tubes subjected to saturation temperatures on the outside should be used to analyse and understand the development of the wetted surface temperatures on the inside of the tube from when flow is developing to when its fully developed.
  -The results from these experimental studies can be confirmed through CFD analyses in extended studies.
  -The Reynolds numbers used to investigate the sensitivity of surface temperatures to inlet temperature and heat input levels can be extended to cover the full laminar flow range for a more through explanation.
- To better understand the development of the bulk fluid temperatures of the water across long lengths of test sections, several compartments of the water bath can be further employed where boiling will occur separately. This will allow for collection of local fluid temperatures flowing along the tube and subsequently the local heat transfer coefficients.
- Further work is also recommended where the surface temperature uniformity is analysed while the test section is being cooled. Refrigerants or other fluids at saturation on the outside of the test section can be employed.

REFERENCES

[1] H.M. Alotaibi, W. Al-Kouz, A. Boretti, Design of a 100 MW Concentrated Solar Power Plant Parabolic Trough in Riyadh, Saudi Arabia, in: E3S Web of Conferences, 2021.

[2] D. Tschopp, Z. Tian, M. Berberich, J. Fan, B. Perers, S. Furbo, Large-scale solar thermal systems in leading countries: A review and comparative study of Denmark, China, Germany and Austria, Applied Energy, 270 (2020) 114997.

[3] B.R.A. Hussein A. M, Kadirgama K, Sharma K. V, Heat transfer enhancement using nanofluids in an automotive cooling system, International Communications in Heat and Mass Transfer, (2014) 195-202.

[4] H. Wagner, The management of heat flow in deep mines, Mining Report, 2013.

[5] Y.A. Cengel, A.J. Ghajar, Heat and Mass Transfer: Fundamentals and Application, 5 ed., McGraw-Hill Education, 2 Penn Plaza, New York, 2015.

[6] A. Faghri, Y. Zhang, J.R. Howell, Advanced Heat and Mass Transfer, Global Digital Press, Columbia, 2010.

[7] F. P. Incropera, D. P. Dewitt, T.L. Bergman, A.S. Lavine, Fundamentals of heat and mass transfer, 6 ed., John Wiley and Sons, Hoboken, 2007.

[8] J.H. Lienhard-IV, J.H. Lienhard-V, A Heat transfer Textbook, 3 ed., Lienhard-V,John H., Cambridge, Massachusetts, U.S.A., 2000.

[9] A.P. Colburn, A Method of Correlating Forced Convection HeatTransfer Data and a Comparison with Fluid Friction, Transaction of the American Institute of Chemical Engineers,, 29 (1933) 174-210.

[10] E.N. Sieder, G.E. Tate, Heat Transfer and Pressure Drop of Liquids in Tubes, Industrial and Engineering Chemistry, 28(12) (1936) 1429-1435.

[11] T.W. Jackson, J.M. Spurlock, K.R. Purdy, Combined free and forced convection in a constant temperature horizontal tube, AIChE Journal, 7(1) (1961) 38-41.

[12] D.R. Oliver, The effect of natural convection on viscous-flow heat transfer in horizontal tubes, Chemical Engineering Science, 17(5) (1962) 335-350.

[13] A.R. Brown, M.A. Thomas, Combined Free and Forced Convection Heat Transfer for Laminar Flow in Horizontal Tubes, Journal of Mechanical Engineering Science, 7(4) (1965) 440-448.

[14] C.A. Depew, S.E. August, Heat Transfer Due to Combined Free and Forced Convection in a Horizontal and Isothermal Tube, J. Heat Transfer, 93(4) (1971) 380-384.

[15] W.W. Yousef, J.D. Tarasuk, Free convection effects on laminar forced convective heat transfer in a horizontal isothermal tube, Journal of Heat Transfer, 104(1) (1982) 145-152.

[16] D. Ndenguma, J. Dirker, J.P. Meyer, Heat transfer and pressure drop in annuli with approximately uniform internal wall temperatures in the transitional flow regime, International Journal of Heat and Mass Transfer, 111 (2017) 429-441.

[17] J. Meyer, J. Olivier, Heat Transfer and Pressure Drop Characteristics of Smooth Horizontal Tubes in the Transitional Flow Regime, Heat Transfer Engineering, 35 (2014).

[18] J. Meyer, Heat Transfer in Tubes in the Transitional Flow Regime, in: The 15th International Heat Transfer Conference, International Heat Transfer Conference, Kyoto, Japan, 2014.

[19] G. Hauke, An Introduction to Fluid Mechanics and Transport Phenomena, Springer Science+Business Media, B.V., Spain, 2008.

[20] M. Everts, J.P. Meyer, Laminar hydrodynamic and thermal entrance lengths for simultaneously hydrodynamically and thermally developing forced and mixed convective flows in horizontal tubes, Experimental Thermal and Fluid Science, 118 (2020) 110-153.

[21] B. Metais, E.R.G. Eckert, Forced, Mixed, and Free Convection Regimes, Journal of Heat Transfer, 86(2) (1964) 295-296.

[22] J.P. Meyer, J.A. Olivier, Heat transfer and pressure drop characteristics of smooth horizontal tubes in the transitional flow regime, Heat Transfer Engineering, 35(14-15) (2014) 1246-1253.

[23] O.C. Eubank, W.S. Proctor, Effect of natural convection on heat transfer with laminar flow in tubes, S.B., Massachusetts Institute of Technology, 1951.

[24] T.D. Bennett, Correlations for the Graetz problem in convection - Part 1: For round pipes and parallel plates, International Journal of Heat and Mass Transfer, 136 (2019) 832-841.

[25] T.D. Bennett, Correlations for the Graetz problem in convection - Part 2: For ducts of arbitrary cross-section, International Journal of Heat and Mass Transfer, 135 (2019) 1327-1334.

[26] K. Stephan, Wärmeübergang und Druckabfall laminarer Strömungen im Einlauf von Rohren und ebenen Spalten, Karlsruhe, 1959.

[27] V. Gnielinski, G1 Heat Transfer in Pipe Flow, in: VDI Heat Atlas, Berlin, Heidelberg : Springer Berlin Heidelberg : Springer, 2010, pp. 691-700.

[28] B. Shome, M.K. Jensen, Correlations for simultaneously developing laminar flow and heat transfer in a circular tube, International Journal of Heat and Mass Transfer, 36(10) (1993) 2710-2713.

[29] Y.S. Muzychka, M.M. Yovanovich, Laminar Forced Convection Heat Transfer in the Combined Entry Region of Non-Circular Ducts, J. Heat Transfer, 126(1) (2004) 54-61.

[30] B. Jacimovic, S. Genic, D. Lelea, Calculation of the Heat Transfer Coefficient for Laminar Flow in Pipes in Practical Engineering Applications, Heat transfer engineering, 39(20) (2018) 1794-1800.

[31] R.K. Shah, A.L. London, Laminar Flow Forced Convection Heat Transfer and Flow Friction in Straight and Curved Ducts - A Summary of Analytical Solutions, in: C. Stanford University, Dept Of Mechanical, Engineering (Ed.), 1971.

[32] H.A. Mohammed, Y.K. Salman, Experimental investigation of mixed convection heat transfer for thermally developing flow in a horizontal circular cylinder, Applied Thermal Engineering, 27(8-9) (2007) 1522-1533.

[33] H.A. Mohammed, A. Campo, R. Saidur, Experimental study of forced and free convective heat transfer in the thermal entry region of horizontal concentric annuli, International Communications in Heat and Mass Transfer, 37(7) (2010) 739-747.

[34] J.P. Meyer, M. Everts, Single-phase mixed convection of developing and fully developed flow in smooth horizontal circular tubes in the laminar and transitional flow regimes, International Journal of Heat and Mass Transfer, 117 (2018) 1251-1273.

[35] N. Islam, U.N. Gaitonde, G.K. Sharma, Mixed convection heat transfer in the entrance region of horizontal annuli, International Journal of Heat and Mass Transfer, 44(11) (2001) 2107-2120.

[36] A.I. Bashir, M. Everts, R. Bennacer, J.P. Meyer, Single-phase forced convection heat transfer and pressure drop in circular tubes in the laminar and transitional flow regimes, Experimental Thermal and Fluid Science, 109 (2019).

[37] M. Everts, J.P. Meyer, Heat transfer characteristics in the laminar and transitional flow regimes for tubes with mixed convestion., in: 9th World Conference on Experimental Heat Transfer, Fluid Mechanics and Thermodynamics, Iguazu Falls, Brazil, 2017.

[38] M. Everts, J.P. Meyer, Flow regime maps for smooth horizontal tubes at a constant heat flux, International Journal of Heat and Mass Transfer, 117 (2018) 1274-1290.

[39] J. Meyer, L. Liebenberg, O. Jonathan, ASHRAE Project 1280-RP: Measurement and Evaluation of Single-Phase Heat Transfer and Pressure Drop Inside Enhanced Tubes for Transition Flow, (2022).

[40] J.P. Meyer, A.I. Bashir, M. Everts, Single-phase mixed convective heat transfer and pressure drop in the laminar and transitional flow regimes in smooth inclined tubes heated at a constant heat flux, Experimental Thermal and Fluid Science, 109 (2019) 109890.

[41] M. Everts, J. Meyer, The Art of Measuring in the Thermal Sciences, 1 ed., CRC Press, 2020.

[42] J.-C. Han, Analytical heat transfer, Taylor & Francis, 2012.

[43] Rohsenow, A Method of Correlating Heat Transfer Data for Surface Boiling of Liquids, ASME Transactions, 74 (1952) 969-975.

[44] J. B. Kitto, S. C. Stultz, Steam: Its generation and use, 41 ed., The Babcock & Wilcox Company, Ohio, USA, 2005.

APPENDICES

A. CALIBRATION

A.1.   Introduction

This appendix gives details to the calibration processes for the Pt100 probes and thermocouples. Also presented are the calibration factors and calibration curves.

A.2.   Pt100 probes

The inlet and outlet temperatures of the water flowing through the test section were measured by two Pt100 probes. These were calibrated to an accuracy of 0.06 °C inside a LAUDA ECO RE 1225 thermostat-controlled bath against a DCS2 Digital thermometer of 0.03 $^{\circ}$C accuracy. The calibration methods and principles detailed by Everts and Meyer [1] were followed in this evaluation. The measuring range was selected between 15°C and 75 $^{\circ}$C and measurements were taken at 5 $^{\circ}$C intervals. Once steady state was reached, an average of 200 measuring points were taken and used for calculations of the calibration factors. Measurements were taken for both increasing and decreasing temperatures to account for hysteresis, ensure a constant curve and increase accuracy. Fig A.1 and A.2 show the Temperature measurements of the Pt100 probes against the digital thermometer. These show that hysteresis was negligible
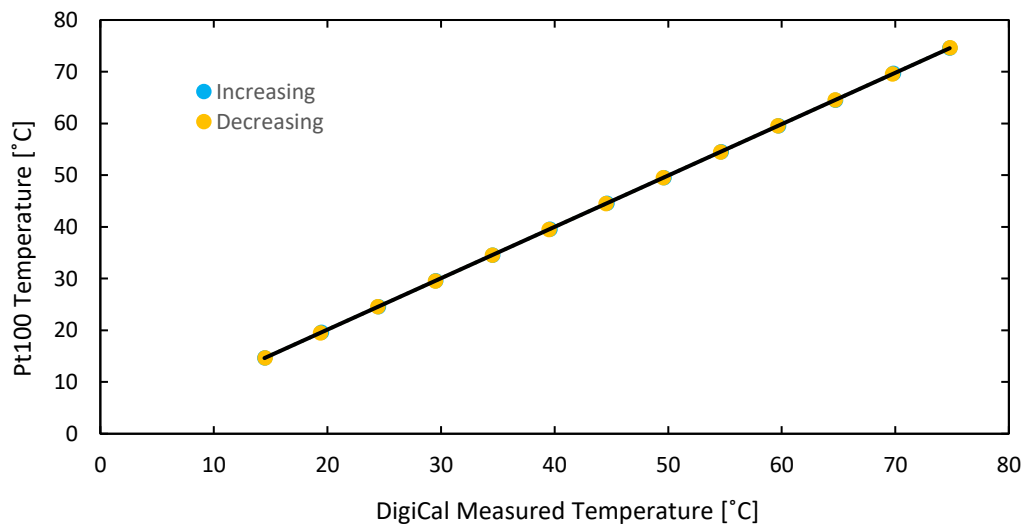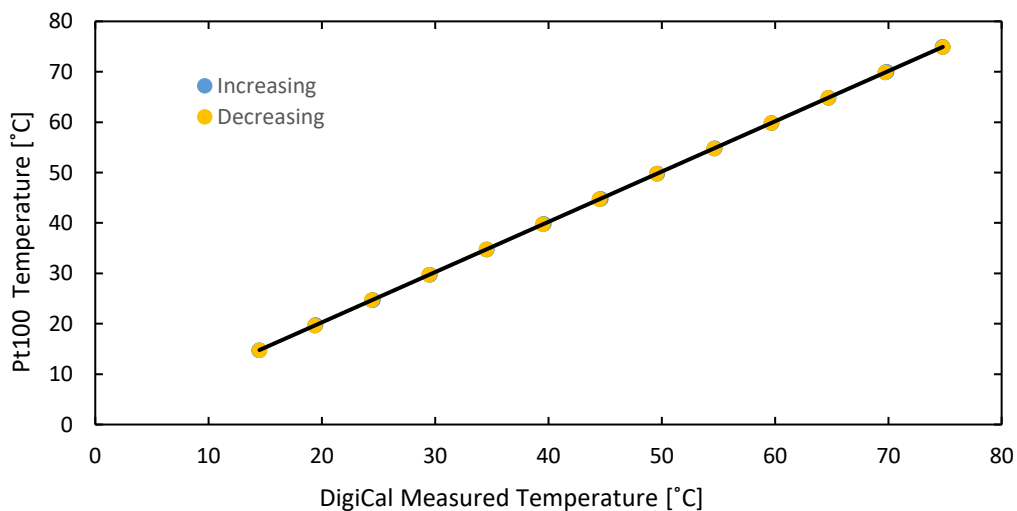

Fig. A.1: Inlet Pt100 probe measurements

Fig. A.2: Outlet Pt100 probe measurements

A.1

The calibration factors, summarised in Table A.1, were obtained using the equation of the line of best fit such that:

$$T_{cal} = \frac{T_{uncal} - c}{m} \tag{A.1}$$

Table A.1: Calibration factors for the inlet and outlet Pt100 probes

Factor	Inlet Pt100	Outlet Pt100
m	0.9932	0.9973
c	0.2725	0.3270

The temperature differences between the measured reference temperatures and the respective uncalibrated and calibrated Pt100 values were thus plotted in Fig. A.3 and Fig. A.4. For the calibrated data to be acceptable, the differences were to within ±0.06 °C lines (the manufacture's specified inaccuracy).
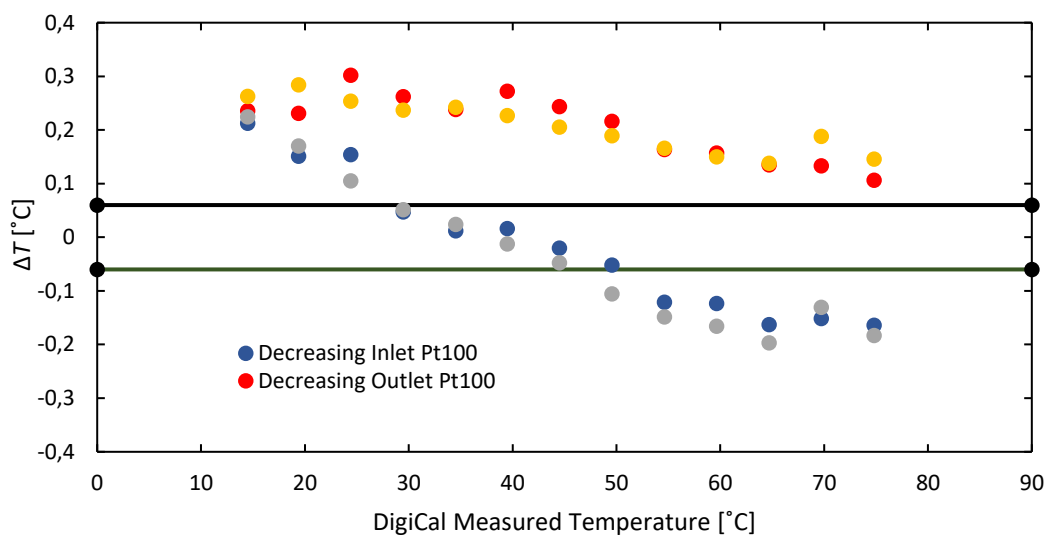

Fig. A.3: Uncalibrated Pt100 probes' measurements uncertainties (upscale and downscale measurements)
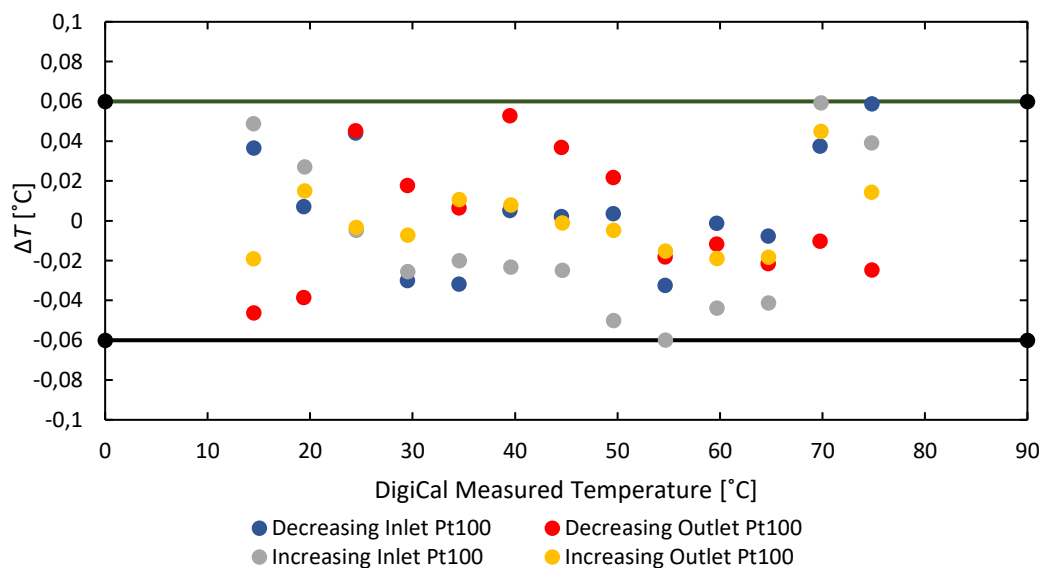

Fig. A.4: Calibrated Pt100 probes' measurements uncertainties (upscale and downscale measurements)

A.2

A.3. Thermocouples

A total of 24 OMEGA T- type thermocouples were attached to the test section across 8 stations (A-H). These thermocouples were calibrated in situ to avoid effects of change in properties at the junctions at soldering them onto the copper tube. The water bath was empty, and the test section was sufficiently insulated during this calibration process. The LAUDA ECO RE 1225 was employed to maintain inlet temperatures at desired levels as calibration was done between 15 °C and 90 °C at 5 °C increments. Steady state conditions were reached first before any readings were taken. An average of 200 measuring points from the two Pt100 probes at the inlet and outlet (used as the reference temperature) as well as the individual thermocouples attached to the test section.

As indicated in Fig. A.5, the calibration factors of the thermocouples were obtained by performing a linear curve fit through the individual thermocouple readings taken and the calibrated Pt100 values. For each thermocouple, the calibrated thermocouple value, T_{cal} could be calculated using Eq. (A.1):
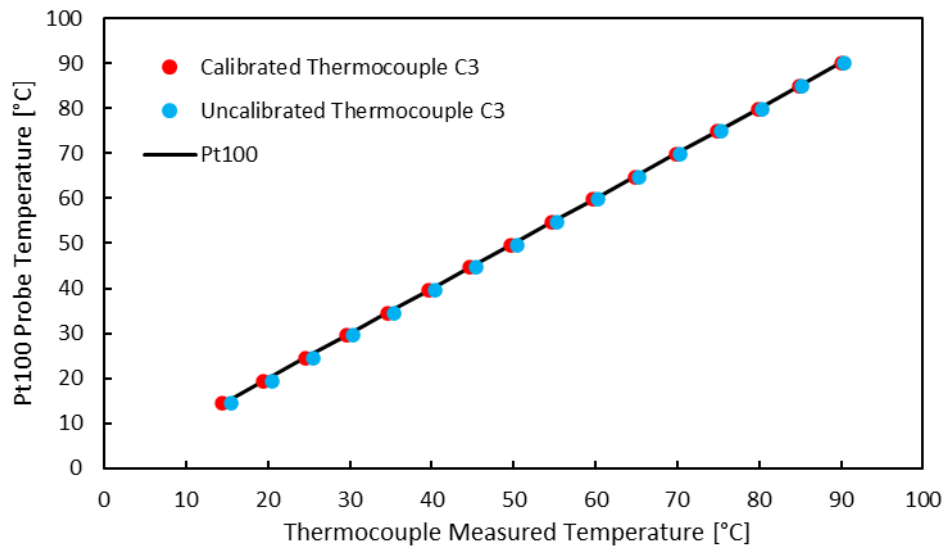

Fig. A.5: Graphical representation of the Pt100 probes temperature measurements compared to the calibrated and uncalibrated temperatures recorded for the thermocouple C3 as an example.

The difference between the measured surface temperatures and the calibrated values were compared together with the reference Pt100 probe measurement in Fig. A.6. The calibration process was considered successful as all the differences between the calibrated values and the reference temperature were within ±0.1 °C (manufacturer's specification). The thermocouples that were suspended in the water bath to measure the saturation temperature were calibrated in the same manner as the Pt100 probes using the Digical thermometer and their uncertainties were within the allowable bounds.

A.3

Table A.2: Calibration factors of the individual thermocouples attached to the test section
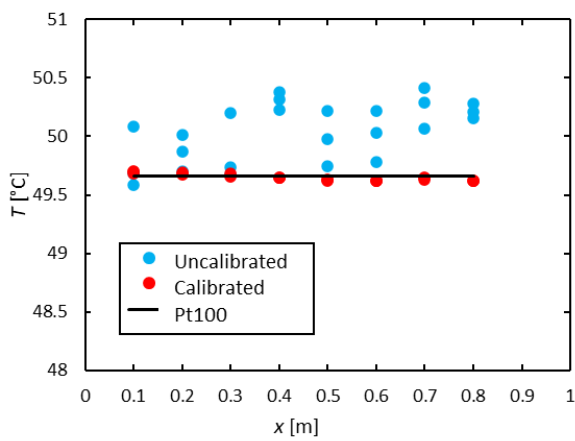
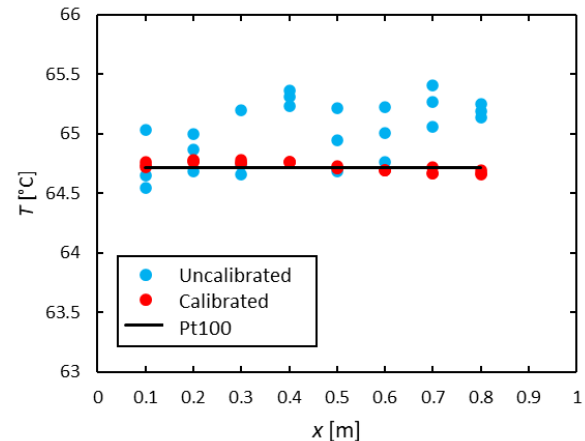| Thermocouple	m	c	Thermocouple	m	c
A1	1.0137	-1.0869	E1	1.0090	-0.8079
A2	1.0114	-0.5544	E2	1.0058	-0.8783
A3	1.012	-0.4790	E3	1.0094	-0.5797
B1	1.0106	-0.8708	F1	1.0071	-0.5271
B2	1.0087	-0.443	F2	1.0071	-0.7785
B3	1.0087	-0.6211	F3	1.0076	-1.0299
C1	1.0071	-0.4060	G1	1.0058	-1.1129
C2	1.0098	-0.4998	G2	1.0054	-0.7491
C3	1.0106	-1.2595	G3	1.006	-0.9880
D1	1.0073	-1.0079	H1	1.0052	-0.8846
D2	1.0079	-0.9797	H2	1.0047	-1.1026
D3	1.0082	-1.1381	H3	1.0078	-0.809
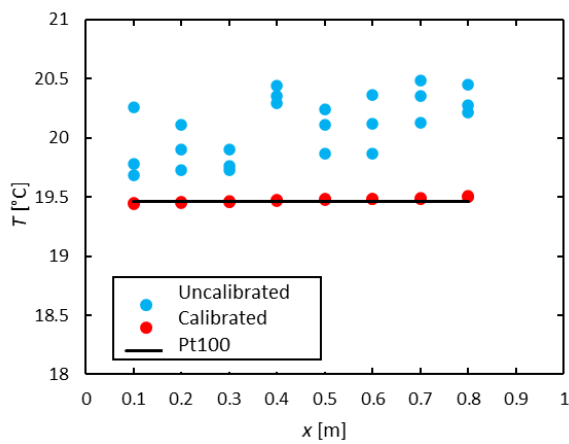
(a)
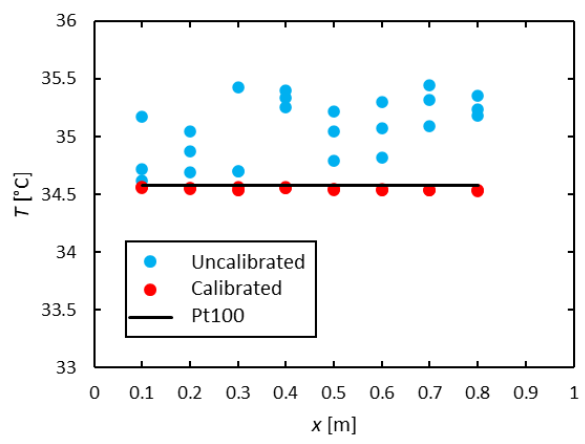
(b)

(c)

(d)

Fig. A.6: Uncalibrated and calibrated thermocouple measurements across the tube's length compared to the Pt100 probe temperature measurements at (a) 19.5 °C (b) 34.6 °C (c) 49.7 °C (d) 64.7 °C

A.4

A.4.   Conclusions

The calibration methods employed for the Pt100 probes and thermocouples were discussed in the preceding sections. The Pt100 probed were calibrated to an accuracy of 0.06 °C inside a LAUDA ECO RE 1225 thermostat-controlled bath against a DCS2 Digital thermometer of 0.03 °C accuracy. The thermocouples were calibrated to an uncertainty of 0.1 °C, in situ, using the calibrated measurements of the two Pt100 probes at the inlet and outlet of the test section.

A.5.   Nomenclature

c	y-intercept	
cal	Calibrated value	
D	Inner diameter	[m]
m	Gradient of curve	
T	Temperature	[°C] or [K]
uncal	Uncalibrated value	
Δ	Change/Difference	

A.6.   List of figures

A.7.   List of tables

A.8.   References

[1] M. Everts, J. Meyer, The Art of Measuring in the Thermal Sciences, 1 ed., CRC Press, 2020

B. UNCERTAINITY ANALYSIS

B.1.   Introduction

An uncertainty analysis was carried out to determine the accuracy of the results of the study. All the relevant uncertainties determined for the different parameters were below 10%. Although each instrument had its own predefined accuracy, the sum of the multiple measurements that are combined in heat transfer coefficients calculations can lead to high uncertainties. The uncertainty for a single point measurement, δx_i with a random error or the precision (P) and the fixed error or the bias (B) could be calculated as:

$$\delta x_i = \sqrt{B_i^2 + P_i^2} \qquad \text{(B.1)}$$

where x_i is the single observation variable [1].

Considering a correlation R with several observation variables R where:

$$R = R(x_1, x_2, x_3 x_4 \dots, x_5) \qquad \text{(B.2)}$$

the uncertainties were determined as:

$$\delta R = \frac{\delta R}{\delta x_i} \delta x_i \qquad \text{(B.3)}$$

where the partial derivative δR is called the sensitivity coefficient. It defines the effect that the uncertainty of a single considered measurement had on the overall uncertainty of the resultant value. Using the root sum method, the partial derivative could be expressed as:

$$\delta R = \sqrt{\left(\frac{\delta R}{\delta x_1}\right)^2 \delta x_1 + \left(\frac{\delta R}{\delta x_2}\right)^2 \delta x_2 + \left(\frac{\delta R}{\delta x_3}\right)^2 \delta x_3 + \dots + \left(\frac{\delta R}{\delta x_n}\right)^2 \delta x_n} \qquad \text{(B.4)}$$

The following sections detail the uncertainty analysis for the various parameters considered. To note is the extensive work that has been done by Dr M. Everts and colleagues at the University of Pretoria to detail the uncertainties of the common parameters used in thermal exchange experimentation and studies [2, 3].

B.2.   Water properties

Popiel and Wojtkowiak [4] detailed equations to calculate the properties of water. The uncertainties associated with their equations are as listed in Table B.1.

Table B.1 Uncertainty of water properties

Property	μ	ρ	k	Pr	c_p	β
Units	[kg/m3]	Kg/m.s	[W/m.K]		[J/kg.K]	
Uncertainty (%)	0.004	0.5	0.04	2	1	2.3

B.3.   Instruments

B.3.1. Pt100 probes

The manufacturer's accuracy of the Pt100 probes was 0.06°C. To avoid any distortions during experimentation, the accuracy the Pt100 probes measurements were calibrated to be within

±006 ˚C using a DCS2 Digital thermometer of 0.03 ˚C.

B.3.2. Thermocouples

Thermocouples attached to the test section were calibrated using methods discussed in Appendix A. The calibrated Pt100 probe readings were the points of reference for the in-situ calibration calculations. The resultant uncertainty of ±0.1 °C was defined as the average bias for each thermocouple.

B.3.3. Flow meter

A single Coriolis flow meter was used to measure the flow rate of water through the test section. It was specified to operate in a range from 5 l/hr up to 108 l/hr. The bias of the flow meters is 0.05% of the full-scale value of the flow meter, therefore an accuracy of 0.054 l/hr was used.

B.3.4. Power supply

3kW EA Electro-Automatic power supplies (nominal rated voltage and current values of 360 V and 15 A respectively) were employed to heat the Constantine heater element in the water bath. The accuracy of the output power was specified <1%, the output Current at < 0.2% while the output voltage was < 0.1%.

B.3.5. Length measurements

A measuring tape with an accuracy of 2 mm was used to take length measurements of the test section, water bath, heater element frame and other components as required.

B.3.6. Diameter of the test section

A vernier caliper with an accuracy of 20 μm was used to measure the inner and outer diameters of the test section which were found to be 11.2 m and 12.5 m respectively.

B.4.   Analysis

B.4.1. Surface temperatures

Each thermocouple station consisted of three thermocouples at 120˚ to each other around the circumference of the round tube. An average of the three was taken as the surface temperature at that position, T_s, such that the uncertainty could be calculated as:

$$\delta T_s = \sqrt{\left(\frac{\delta T_{s1}}{3}\right)^2 + \left(\frac{\delta T_{s2}}{3}\right)^2 + \left(\frac{\delta T_{s3}}{3}\right)^2} = 0.0058\,°\text{C} \qquad (\text{B.5})$$

B.4.2. Cross-sectional area of test section

Since the cross-sectional area of the test section was calculated as:

$$A_c = \frac{\pi}{4}D^2 \qquad (\text{B.6})$$

The associated uncertainty could be calculated as

$$\delta A_c = \sqrt{\left(\frac{\delta A_c}{\delta D}\delta D\right)^2}$$

$$\delta A_c = \frac{\pi D}{2}\delta D \qquad (\text{B.7})$$

B.2

$$\delta A_c = 3.77 \times 10^{-7} \text{ m}^2$$

B.4.3. Heat transfer area

The heat area of the tube was calculated as:

$$A_s = \pi D L \tag{B.8}$$

The uncertainty associated to the heat transfer area could then be calculated as:

$$\delta A_s = \sqrt{\left(\frac{\delta A_s}{\delta D}\delta D\right)^2 + \left(\frac{\delta A_s}{\delta L_{heated}}\delta L_{heated}\right)^2} \tag{B.9}$$

For the full 1m length of the tube, the uncertainty was calculated to be δA_s = 0.094 mm

B.4.4. Heat input into the water

The heat input into the water was defined as:

$$\dot{Q} = \dot{m}c_p(T_{out} - T_{in}) \tag{B.10}$$

The uncertainty could then be reduced to:

$$\delta\dot{Q} = \sqrt{\left(c_p(T_{out} - T_{in})\delta\dot{m}\right)^2 + \left(\dot{m}(T_{out} - T_{in})\delta c_p\right)^2} \tag{B.11}$$

B.4.5. Heat transfer coefficient

The uncertainty of the heat transfer coefficient could be calculated as follows:

Since:

$$h = \frac{\dot{q}}{T_s - T_m} \tag{B.12}$$

Therefore:

$$\delta h = \sqrt{\left(\frac{\partial h}{\partial \dot{q}}\delta\dot{q}\right)^2 + \left(\frac{\partial h}{\partial T_s}\delta T_s\right)^2 + \left(\frac{\partial h}{\partial T_m}\delta T_m\right)^2}$$

$$\delta h = \left(\frac{1}{T_s - T_m}\delta\dot{q}\right)^2 + \left(-\frac{\dot{q}}{(T_s - T_m)^2}\delta T_s\right)^2 + \left(\frac{\dot{q}}{(T_s - T_m)^2}\delta T_m\right)^2 \tag{B.13}$$

B.4.6. Nusselt number

The Nusselt Number could be calculated as

$$Nu = \frac{hD}{k} \tag{B.14}$$

Thus, the associated Nusselt number uncertainty could be reduced to:

$$\delta Nu = \sqrt{\left(\frac{D}{k}\delta h\right)^2 + \left(\frac{h}{k}\delta D\right)^2 + \left(-\frac{hD}{k^2}\delta k\right)^2} \tag{B.15}$$

For all Nusselt numbers calculated, the uncertainties were below 10%.

B.4.7. Reynolds Number

The Reynolds Number was calculated as:

$$Re = \frac{\dot{m}D}{\mu A_C} \tag{B.16}$$

The Reynolds number uncertainties were approximately 2% and could be calculated using:

$$\delta Re = \sqrt{\left(\frac{\delta Re}{\delta \dot{m}}\delta \dot{m}\right)^2 + \left(\frac{\delta Re}{\delta D}\delta D\right)^2 + \left(\frac{\delta Re}{\delta \mu}\delta \mu\right)^2 + \left(\frac{\partial Re}{\delta A_c}\delta A_c\right)^2}$$

$$\delta Re = \sqrt{\left(\frac{D}{\mu A_c}\delta \dot{m}\right)^2 + \left(\frac{\dot{m}}{\mu A_c}\delta D\right)^2 + \left(-\frac{\dot{m}D}{\mu^2 A_c}\delta \mu\right)^2 + \left(-\frac{\dot{m}D}{\mu A_c^2}\delta A_c\right)^2} \tag{B.17}$$

B.5.   Results

The laminar flow regime is associated with very low flow rates such that the uncertainty of the flow rates and thus the Reynolds numbers could have notable impact on the uncertainty of results. The Reynolds number uncertainty also relied on the measurement of the tube diameter, the dynamic viscosity and cross-sectional area, all which are parameters that needed their uncertainties determined as well. When the Reynolds number was increased, its uncertainty increased slightly as shown in Fig B.1
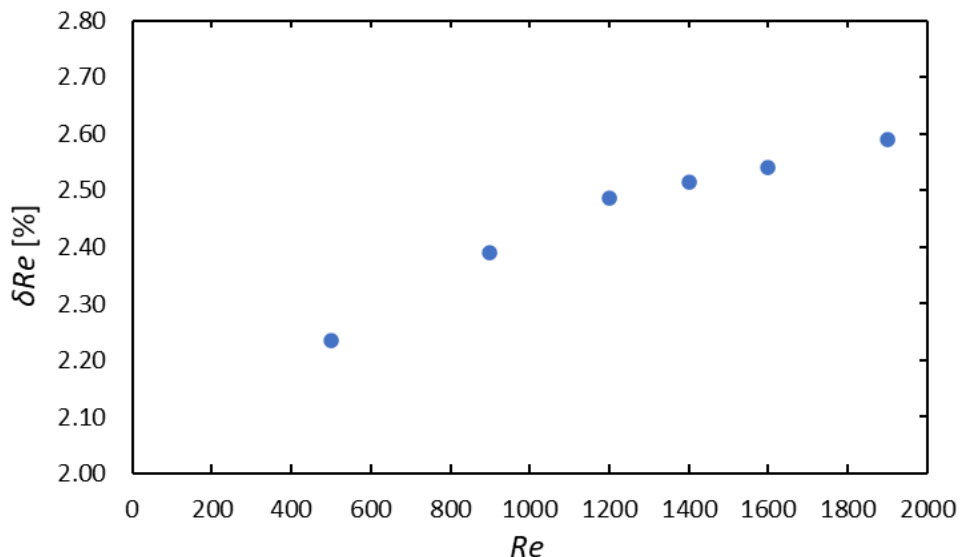

Fig. B.1: Variation of the Reynolds number uncertainty as it is increased

However, the uncertainties of the Nusselt numbers decreased with an increase in the mass flow rates due to the increased temperature difference between the surface of the test section and the bulk fluid (as indicated in Fig. 5.2). For the same reason the heat transfer coefficients uncertainties also

B.4

decreased with an increase in tube inlet temperature (Fig. B.2) since the bulk fluid temperature would be closer to the surface temperatures.
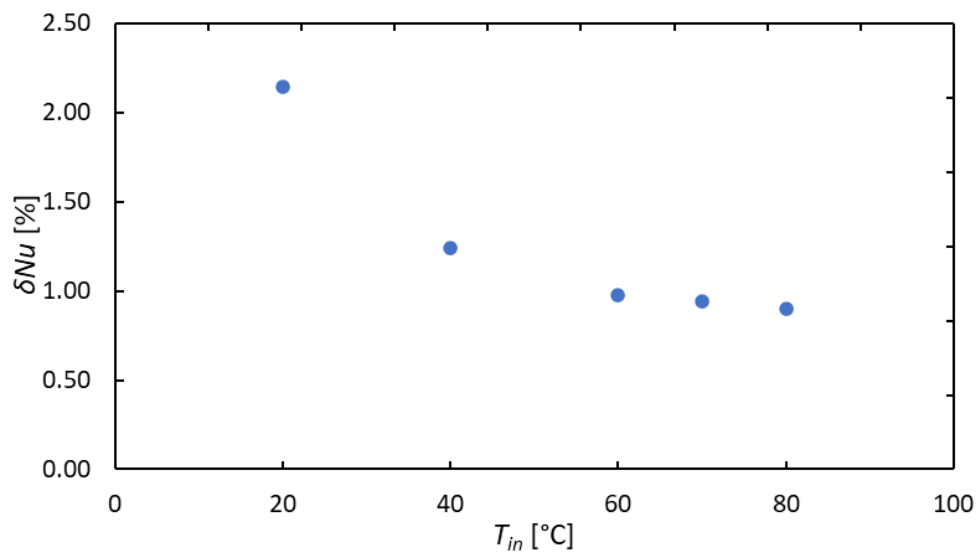

Fig. B.2: Variation of the Nusselt number uncertainties for increasing inlet temperatures

On the other hand, the average Nusselt number uncertainties increased with an increase in electrical heat input (Fig A.3) due to the increase in the temperature gradients along the tube length.
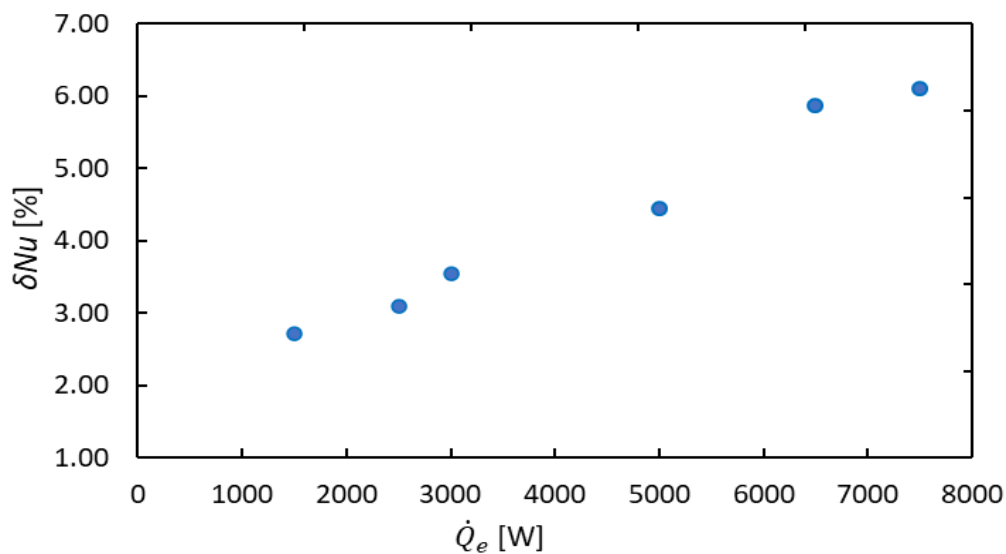

Fig. B.3: Variation of the Nusselt number uncertainties for increasing power input

The local Nusselt number uncertainties were high, up to 17%, due to higher uncertainty from the mean fluid temperatures along the test section's length which are obtained analytically. However, the resultant uncertainties on most measured and analysed parameters were within acceptable limits.

B.6.   Conclusions

This Appendix detailed the uncertainty analysis of the various parameters considered. The supplier's specified uncertainties were considered for the directly measured values. Details were also given on the procedures to follow in calculating the combined uncertainties for Nusselt Numbers, Reynolds numbers and other relevant equations considered in this heat transfer study.

B.7. Nomenclature

B.7.1. Symbols

A	Area	[m^2]
c_p	Constant pressure specific heat	[J/kgK]
D	Diameter	[m]
h	Convection heat transfer coefficient	[W/m^{2}K]
I	Current	[A]
k	Thermal conductivity	[W/m.K]
L	Length	[m]
$\dot{m}$	Mass flow rate	[kg/s]
$\dot{Q}$	Heat input	[W]
$\dot{Q}_e$	Electrical power input	[W]
$\dot{q}$	Heat flux	[W/m^2]
T	Temperature	[°C or K]
V	Voltage	[V]
x	Local value/ Distance between two points	[m]
x_i, B, P, R	Parameters used in correlations	
Nu	Nusselt number	
Pr	Prandtl number	
Re	Reynolds number	
μ	Dynamic Viscosity	[kg/m.s]
ρ	Density	[kg/m^3]
v	Kinematic Viscosity	[m^2/s]
β	Thermal Expansion	

B.7.2. Subscripts

ave	Average
b	Bulk
e	Electrical
exp	Experimental
i	Inner
in	Inlet
lm	Logarithmic mean value
max	Maximum
min	Minimum
n	Experimental constant
o	Outer
out	Outlet
s	Surface
sat	Saturation

B.8. List of figures

B.6

B.9. List of tables

B.10.   References

[1] P.F. Dunn, Measurement and Data Analysis for Engineering and Science, 2nd ed., 2010.

[2] M. Everts, J. Meyer, The Art of Measuring in the Thermal Sciences, 1 ed., CRC Press, 2020

[3] M. Everts, Heat transfer and pressure drop of developing flow in smooth tubes in the transitional flow regime, Master's dissertation, University of Pretoria, Pretoria, 2014.

[4] C.O. Popiel, J. Wojtkowiak, Simple formulas for thermophysical properties of liquid water for heat transfer calculations [from O°C to 150°C], Heat Transfer Eng, Vol. 19(3), pp. 87-101, 1998.